Enrico Lanza

XXX II Cycle

PhD in Life Sciences

SAPIENZA
Università di Roma

C. elegans based strategy for high-throughput early cancer detection through urine analysis

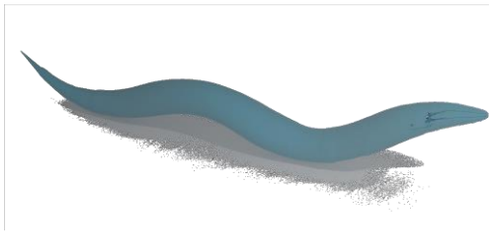

Candidate
Enrico Lanza

Supervisor
Prof. Alessandro Rosa

Tutor
Prof. Giancarlo Ruocco
Dr. Viola Folli

PhD Program in Life Sciences

XXXII Cycle

SAPIENZA
Università di Roma

PhD Programme in Life Sciences

XXXII Cycle

C. elegans based strategy for high-throughput early cancer detection through urine analysis

Candidate
Enrico Lanza

Supervisor
Prof. Alessandro Rosa

Tutor
Prof. Giancarlo Ruocco
Dr. Viola Folli

Coordinator
Prof. Marco Tripodi

C. elegans based strategy for high throughput early cancer detection through urine analysis

Enrico Lanza

October 2019

Contents

1 Introduction **5**

2 Setting-up the experimental workflow **17**
2.1 Chemotaxis assays and urine collection protocol . . . 18
2.2 Different microfluidic devices 21
2.3 Different chemosensory neurons 23
2.4 Sensitivity as a function of odorant concentration . . 28
2.5 Optimization for high-throughput experiments 29

3 Results **36**

4 Discussion and conclusion **48**

5 Materials and Methods **53**
5.1 *C. elegans* strains 53
5.2 Optical setup 54
5.3 The microfluidic chip 57
5.4 Microfluidic device fabrication 60
5.5 Odorant delivery system 63
5.6 Computer controls, GUI and post-processing 65

5.7 Paralyzing solution administration and stocking . . . 68
5.8 Buffer solution preparation 69
5.9 Urine solution preparation 69
5.10 *C. elegans* preparation 69
5.11 Urine sample collecting and stocking 71
5.12 Urine testing 71

6 Troubleshooting **73**
6.1 Problems related to the microfluidic environment . . 73
6.2 Problems related to the *C. elegans* 77
6.3 Problems related to the urine samples 79

A Calcium Imaging Protocol **87**

B Ethics committee approval **90**

1 Introduction

Caenorhabditis elegans was introduced as a developmental model in neurobiology in 1963 by Sydney Brenner, who later started research also in molecular and developmental biology on this nematode [1]. It has since been widely studied as a model organism thanks to many aspects, which include ease of cultivation, invariant cell number and genetic tractability, making it a practical tool to study the same biological processes worldwide. With a three-week long life span, this nematode is about 1 mm long and lives in temperate soil environments. The adult hermaphrodite *C. elegans* (see figure 1), which has an occurrence of 99.9% in the individuals of the species, consists of only 959 cells with stereotypical functions and fixed lineage. Lacking a circulatory and respiratory system, its unsegmented and bilaterally symmetrical anatomy comprises mouth, pharynx, intestine, gonad and collagenous cuticle. The optical transparency of these tissues facilitates visual inspection, and the relatively low number of neurons (namely 302) involved in a rich variety of behavioural responses make it also particularly suited for neuroscience.

Because of these properties, *C. elegans* has been subject to various studies, describing biological phenomena at all levels, ranging from molecular processes to collective behaviours. In the years that followed its introduction in the scientific world, we have collected so much information on this roundworm that today, its entire cell lineage has been known for more than 35 years [2, 3], and we have an almost complete knowledge of the structure of its nervous system, whose reconstruction started in the '80s with a series of electronic micrographs [4], later updated multiple times [5, 6, 7].

One of the most interesting properties of this nematode for the purpose of the study presented in this work, is related to its olfaction capabilities. Since *C. elegans* lacks long range sensory mechanisms, like vision and audition, its sense of smell compensates for this deficit by featuring a high complexity, in spite of the low number of neurons involved in smelling. To have an idea of how developed its olfaction is, it is worth to notice that about one thousand of genes of *C. elegans* encode GPCRs (G protein coupled receptors). GPCRs

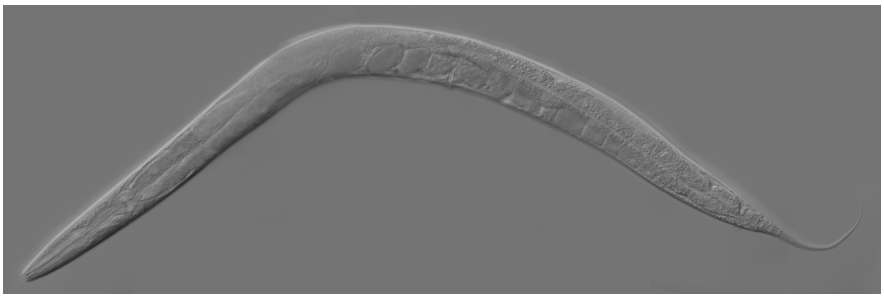

Figure 1: Transmission image of an adult hermaphrodite *C. elegans* with visible eggs [8]. *C. elegans* is a nematode that is about 1 mm long and completely transparent. This image is licensed under the Creative Commons Attribution-Share Alike 2.5 Generic license (https://creativecommons.org/licenses/by-sa/2.5/legalcode).
Author: the original uploader was Kbradnam at English Wikimedia (Original text: Zeynep F. Altun, Editor of www.wormatlas.org).

are seven-pass-transmembrane domain receptors that activate internal signal transduction pathways upon detection of molecules outside the membrane. A great fraction of these proteins is predicted to act as olfactory receptor. This number is very close to the amount of GPCRs encoded in the DNA of mammals with a highly developed sense of smell, like dogs and rodents. However, mammals have billions of billions of neurons, while *C. elegans* has only hundreds of such cells, which are generally organized in bilaterally symmetric pairs (left and right counterparts with structural and functional similarities). In mammals, each olfactory neuron expresses only one or a few chemoreceptors of the same gene family [9, 10]. This means that the neuronal trace of odour perception at a sensory level is thus the subset of activated neurons, because their activation is odour specific [11]: a group of the activated subset will respond to a specific property of the sensed chemical, while others respond to other properties. On the other side, *C. elegans* chemoreceptors for environmental chemicals are thought to be expressed in 30 neurons in total (see figures 2 and 3), which co-express many different receptors and are thus responsible for perception of a wide array of different odorants [12] (see table 1). Additionally, each receptor may bind different

molecules. In this case, the activation pattern of the olfactory neurons is again a signature of the sensed chemical, but the activation of a single neuron may not be odorant-specific as for mammals. This makes it generally difficult to associate a specific odour to a specific receptor in the nematode. Among the olfactory neurons of *C. elegans*, 6 are responsible for olfaction and 24 for gustation ([13]): in chemotaxis assays, the perception of odorants placed above the nematodes was driven by the three pairs of olfactory neurons named AWA, AWB and AWC. The difference between olfaction and gustation is related to the perception radius and concentration [14]. The sense of taste is related to short range sensation at micromolar to millimolar concentrations, while olfaction has a broader range and is sensitive to nanomolar concentrations [13]. Figure 4 shows an outline of the chemical connectivity of the olfactory circuit in the head of *C. elegans*, together with interneurons and motor neurons that allow to select and carry out chemotactic behaviour.

While the low number of neurons facilitates the identification of those ones enabling the perception of specific odorants, the fact that these sensory cells respond to different odorants shifts the difficulty of the studies related to olfaction in *C. elegans* to a molecular level: it is usually very hard to associate an odour with a specific receptor. This means that instead of silencing a neuron to assess its involvement in the sensation of a specific odorant, it is required to silence a specific gene. An other difficulty related to the coexpression of GPCRs is that they sometimes undergo the so-called heterodimerization process. During heterodimerization two GPCRs form a complex that features either a different affinity to the same odorant, and/or affinity for an odorant that would not be sensed otherwise, or even a higher signal transduction probability. When studying such phenomena, the silencing of just one of the GPCRs involved in odor-specific sensation would imply a loss of function leading to the erroneous conclusion that the protein encoded by the silenced gene is the only mediator of the process, when in fact, it is not true.

The interest in *C. elegans* olfaction and gustation is related to its high sensitivity, given its impressive detection abilities that reach nanomolar concentrations for olfaction. Thanks to these capabilities,

a team of Japanese researchers led by Hirotsu demonstrated in 2015 the impressive ability of *C. elegans* to detect cancer metabolites in urine samples [15]. Japan is a country with one of the highest consumption of fish, which often reaches the tables uncooked. When not properly treated, raw fish usually contains a parasite called *Anisakis Simplex*. This nematode can infest the gastrointestinal tract of humans (a pathology named *Anisakidosis*), leading to intestinal perfo-

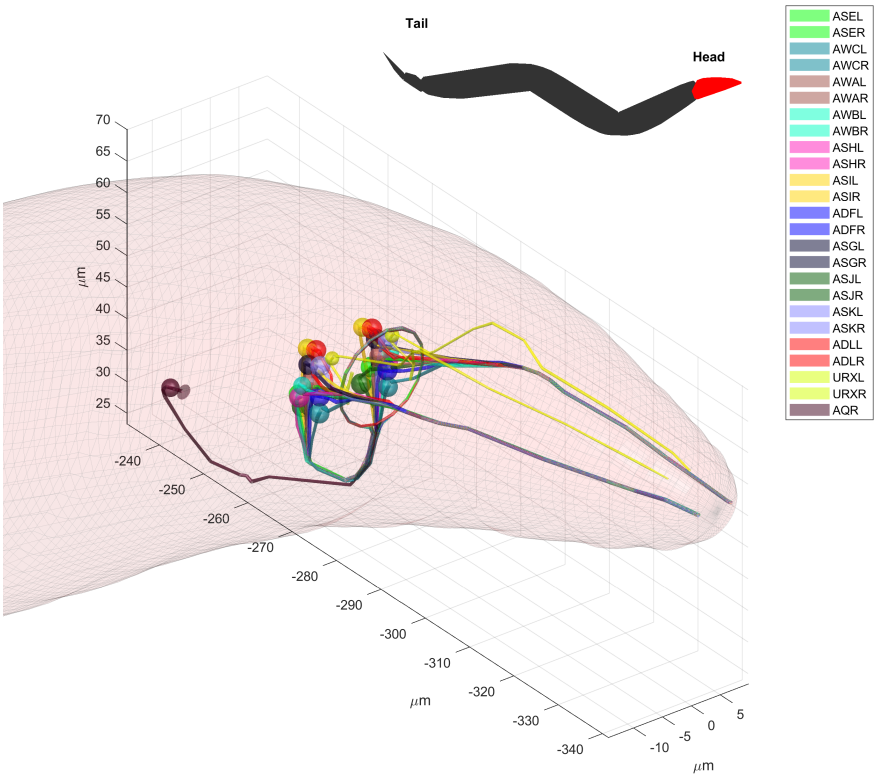

Figure 2: Chemosensory neurons in the head. The main image refers to the head part of the body, highlighted in red in the above sketch. In this region, there are 25 chemosensory neurons, whose morphology is represented in the main graph according to a colour coded legend for bilaterally symmetric pairs. Most of these neurons have processes that reach the most anterior part of the body, to sense surrounding chemicals.

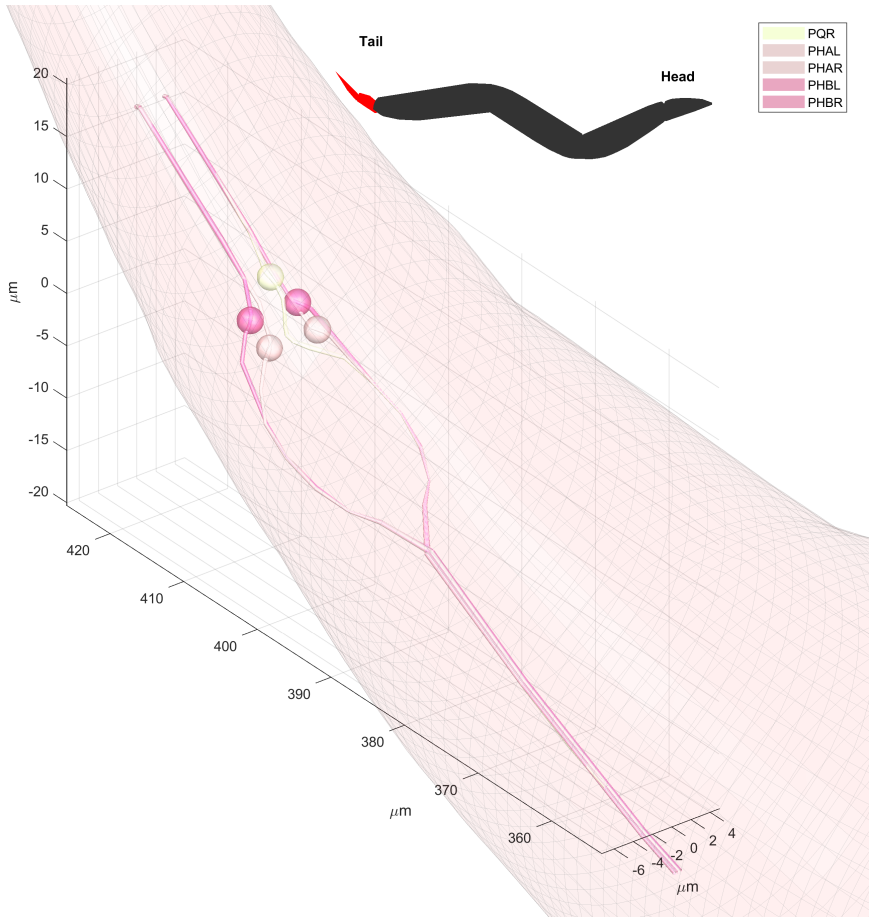

Figure 3: Chemosensory neurons in the tail. The main image refers to the tail part of the body, highlighted in red in the above sketch. This region presents 5 chemosensory neurons with processes. Their morphology is represented in the main graph according to a colour coded legend for bilaterally symmetric pairs

ration in the worst cases. According to a meta-analysis carried out by Hirotsu and his collaborators, from the '70 up until our days, there have been many reported cases of cancer patients in Japan undergoing surgical operation while suffering from *Anisakidosis* as well. In most of these cases, the medical records report something remarkable: the parasites tended to gather on metastases present in the infested tis-

sues. Hirotsu and his collaborators decided thus to investigate this behaviour, but chose to test it on an other, less dangerous nematode, namely *C. elegans*. They found out that *Anisakis* was not the only one showing a chemotactic behaviour towards cancerous tissue. Chemotaxis is the tendency of an organism to migrate towards preferred environments, led by chemical cues. The team showed how *C. elegans* young adults placed in a neutral environment move towards drops of biofluids collected from cancer patients if present. All cancer types involved in their studies related to the gastrointestinal tract with the addition of breast cancer, while the tested biofluids were blood derived fluids and urine samples. On the other side, the same biofluids collected from healthy subjects elicit avoidance. The striking fact

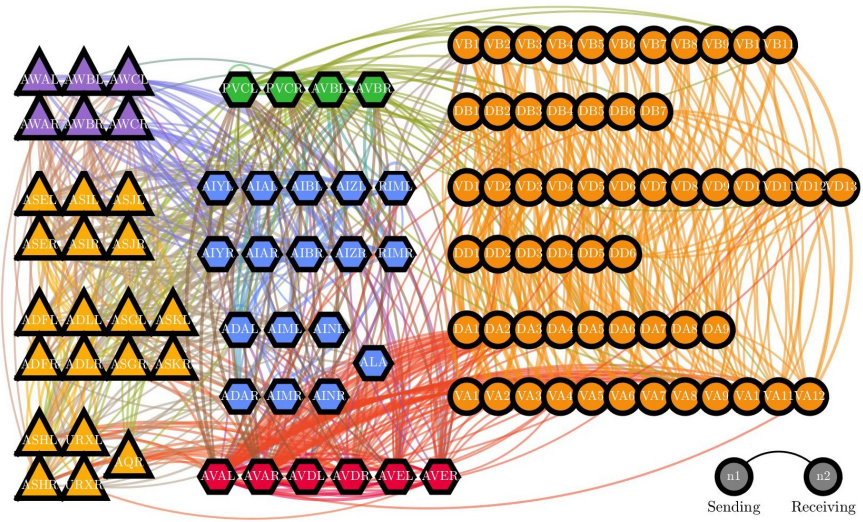

Figure 4: Outline of the chemical connectivity of the olfactory circuit in the head of *C. elegans* together with interneurons and motor neurons that allow to select and carry out chemotactic behaviour. Triangles represent chemosensory neurons (purple for volatile olfaction, yellow otherwise), blue hexagons represent interneurons, green hexagons represent forward-movement promoting neurons, red ones backward-movement promoting neurons and orange circles motor neurons. The direction of the synapses is defined by the bottom right sketch.

about these behaviours, is that *C. elegans* has an extremely high accuracy in discriminating between urine samples from healthy subjects, leading to avoidance, and samples from cancer patients, which lead to attraction. In chemotaxis assays, the reported accuracy reached a value of 93%, which is higher than the accuracy related to the usual biomarkers used for the same types of cancer [16, 17]. This ability leads to the idea that *C. elegans* may offer an advantageous way to detect cancer presence from easily collectible fluids, in spite of the

AWA	**AWB**	**AWC**
sra-13	sra-23	sra-13
sra-17	srab-1	srab-16
(srab-7)	srab-4	srd-5
srab-9	srab-16	srd-17
srab-13	srab-24	sre-4
(srj-21)	srd-11	sri-14
(srj-22)	srd-23	(srj-21)
srt-7	sre-43	(srj-22)
srv-34	srh-211	srsx-3
srx-47	srsx-3	srsx-5
str-261	sru-38	srsx-37
odr-10	srv-5	srt-7
	srx-14	srt-28
	srxa-1	srt-29
	srz-27	srt-45
	str-1	srt-47
	str-44	srx-1
	str-163	str-2
	str-220	str-130
		str-199

Table 1: GPCRs reported to be expressed by the three chemosensory neurons AWA (12), AWB (19) and AWC (20) [12]. Gene in parenthesis are identified on the basis of position and morphology and are still not confirmed with neuron-specific reporter. Many other GPCRs are expected to be reported in these neurons.

low specificity.

Although being supported by previous studies of sensitivity towards cancer metabolites with dogs and rodents [18, 19, 20, 21], gas mass inspection of the samples collected by Hirotsu did not show significant results. This is due to the fact that body fluids, and urine samples in particular, are a complex collection of metabolites and waste products coming from the whole body, showing dramatic differences from individual to individual. The variability makes it very difficult to associate specific concentration profiles to specific pathologies, although, in principle, it is not impossible. Another drawback of the gas mass inspection is related to its sensitivity, which reaches micromolar concentrations, whereas *C. elegans* is able to detect even nanomolar differences.

Based on the previous considerations, the aim of this work is to validate the response of *C. elegans* towards cancer metabolites in urine samples and to investigate the mechanisms underlying this binary response, possibly enhancing the detection accuracy. This study is also part of a wider project aimed at dissecting the molecular processes involved in such a high sensitivity. Indeed, attraction or repulsion of *C. elegans* is the mere consequence of specific neuronal activation. When it comes to detecting the activation of neurons, calcium indicators [22] are one of the most powerful tool in neurosciences, especially advantageous in the case of the transparent body of *C. elegans*. These proteins can be genetically encoded in a host DNA [23, 24]. When expressed, calcium indicators diffuse in either the cytoplasm or the nucleus and show calcium dependent fluorescence properties. This means that upon specific light stimulation followed by calcium binding, these proteins emit a frequency specific fluorescence radiation, whose intensity is proportional to the concentration of calcium in the surroundings. Figure 5 shows the outline of the crystal structure of the green calmodulin protein (GCaMP) in calcium bound state and calcium free state as reported in [25]. Because neuronal activity is calcium dependent, by expressing these proteins in specific neurons, it is possible to indirectly measure the activity of the targeted neuron by shining a light on the nematode. A strain expressing calcium indicators in chemosensory neurons al-

lows to identify sensory neurons responding to a specific odorant, narrowing down the subset of the olfactory circuit to target in the experiments. Once the subset of odour sensitive neurons is identified, it is possible to focus on this group of cells when assessing the accuracy of the *C. elegans* urine-discriminating behaviour. Furthermore, checking the response at the level of sensory neurons is a good way to enhance the reported accuracy based on chemotaxis tests, which is a behavioural output and therefore subject to contingent stimuli. In fact, the outcome of a chemotactic test may be affected for example by room temperature, vibrations or other factors. These tests are thus usually conducted in a very controlled environment. Conversely, calcium indicators allow to detect the information fed to the nervous system as soon as it is detected and generated by the odour sensitive neurons, regardless of how it will affect the nematodes behaviour. At a neural network level, a chemotactic assay is a downstream measurement, while calcium imaging is an upstream one, and therefore necessarily more reliable.

In the experiments aimed at testing the nematode response to chemical stimuli at a neuronal level, we employ a microfluidic device. It is a chip made of polydimethylsiloxane (PDMS) able to confine the animals in the field of view of the camera and to spatially direct the delivery of chemical stimuli. Devices like this have been widely employed to constrain gas and fluids at capillary regimes in controlled environments [26]. They have been extensively used to study many problems related to various scientific fields, such as physics, chemistry, biochemistry, nanotechnology, biotechnology and engineering. There are many examples of microfluidic device usage also in experiments dealing with *C. elegans*, involving chips of various designs and different purposes [27]. Some of these devices are suited for animal handling and manipulation ([28]), others for immobilization [29], for behavioural assays [30], for high-throughput imaging and screening [31], and even for laser microsurgery [32]. In this study, we employ chips suited to collect signals from calcium indicators in multiple worms simultaneously, while exposing them to chemical stimuli. An example of these kind of devices is in [33] and [34].

To go deeper in the description of the mechanisms involved in the

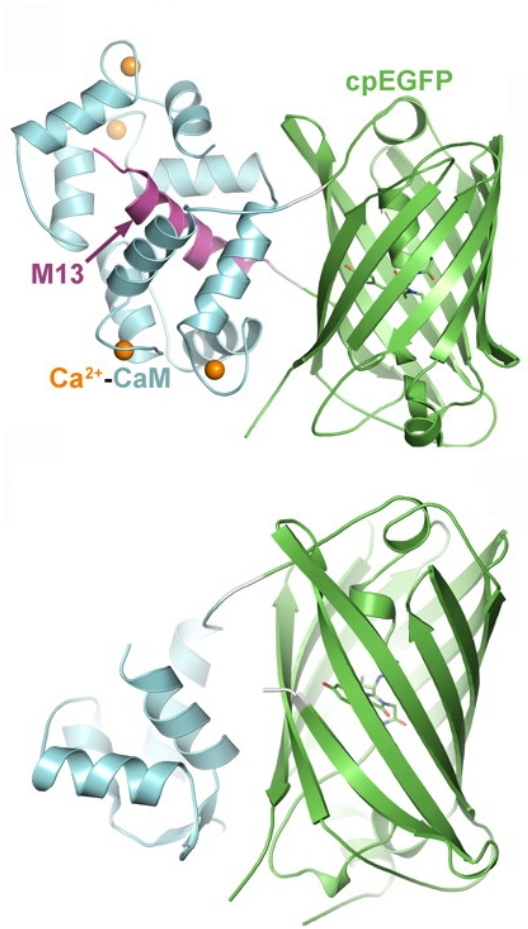

Figure 5: Outline of the crystal structure of the green calmodulin protein (GCaMP) in calcium bound state (top) and calcium free state (bottom) as obtained in [25]. The EGFP chromophore is represented in green, calmodulin in blue, the M13 peptide in purple and calcium ions in orange. The image (available on https://commons.wikimedia.org) is licensed under the Creative Commons license (https://creativecommons.org/licenses/by/3.0/legalcode).
Authors: Akerboom, Rivera, Guilbe, Malavé, Hernandez, Tian, Hires, Marvin, Looger, Schreiter ER.

generation of the chemotactic response of *C. elegans*, the project includes the study of the phenomenon at a molecular level. Olfactory neurons activate when a molecule binds a receptor placed on the cell membrane. For the particular case of cancer metabolites detection in urine samples, we do not know which molecules or metabolites bind to which receptors. To have an idea of the involved metabolites, we can single out the receptors required for the detection by silencing one by one GPCRs encoding genes reportedly expressed by the odour responsive neurons (once these neurons are identified through calcium imaging) and assessing their response again. In case there are no already available knock-out strains, which can be bought at the Caenorhabditis Genetics Center (CGC, University of Minnesota), the silencing can be achieved through gene editing techniques like CRISPR-Cas9.

In parallel with the identification of the involved GPCRs (which add up to 6 out of 20 for now), we can build predictive models through computational biology techniques. This is necessary because purifying GPCRs is a very difficult process, so, a good step to start this investigation is to identify possible bindings through computational models. With a list of GPCRs involved in the *C. elegans* chemical response, we can create a list of putative ligands interacting with these receptors. On the other side we can apply gas mass spectrometry to look for metabolites with the same chemo-physical properties of the ligands identified as putative binding molecules through the computational approach. It is worth to notice that there is no guarantee that the resolution of gas mass spectrometry, which is in the micromolar range, is able to identify the involved ligands in urine samples. However, we can run multivariate analysis to look for a panel of metabolites that best discriminates between the two populations of urine samples: healthy and unhealthy ones. Among the molecules included in the discriminating panel of metabolites, there will be some sharing similar chemo-physical properties with the ligands identified through computational biology. These ones will be the putative metabolites binding to the GPCRs involved in the urine related chemotactic behaviour. To validate that their interaction is involved in urine discrimination, we can perform single molecules

chemotaxis assays in conjunction with gene silencing of the GPCRs that bind with the metabolites found in urine samples. In this way, the long list of GPCRs can be narrowed down to tens, or even just a few of them in the best case. We can additionally perform molecular dynamics on these GPCRs, to predict the binding sites, and the binding affinity. Therefore, by the end of this project, we will have a list of GPCRs involved in the impressive cancer metabolites discriminating behaviour of *C. elegans*.

In the framework of the aforementioned project, my contribution, which is also the subject of this work, was to design and build an experimental setup for calcium imaging to test the *C. elegans* chemical response towards urine samples from breast cancer patients and healthy individuals by monitoring the neuronal activity of olfactory neurons. The result of my work is the validation and the calculation of the accuracy related to the ability of *C. elegans* to discriminate between samples from cancer patients and healthy ones.

2 Setting-up the experimental workflow

As described in the previous section, the aim of this project is to design and build an experimental setup to test the *C. elegans* chemical response towards urine samples from breast cancer patients and healthy individuals. To do this, we applied calcium imaging techniques on *C. elegans* strains expressing calcium indicators on chemosensory neurons putatively involved in cancer metabolites sensing. This kind of experiments requires an optical setup to record images at a magnification that allows to imagine head neurons, whose size is typically in the range of microns for nematodes. It additionally needs a transmission channel to determine the animals location and focal plane, and a fluorescence channel with excitation wavelength λ=485 nm. The latter is strictly related to the excitation wavelength of the calcium indicator expressed by the nematodes. It produces a light that excites calcium indicators, a phenomenon followed by the radiative decay of the fluorophore to the ground state. In this work, we use strains expressing GCaMP3 [35], a blue-light excitable calcium indicator. The fluorescent radiation produced by the radiative decay represents the signal that we want to collect in a systematic way. Because intracellular calcium levels are affected by neuronal dynamics, such a signal represents an indirect measurement of neuronal activation. Another element of the setup that may crucially influence the outcome of the experiments is the microfluidic device, needed to keep the animals in the field of view of the camera and to spatially direct the delivery of chemical stimuli. These devices have been extensively employed to control fluids in constrained environments at capillary regimes [36]. Their design and fabrication processes have already been standardized [37], but need to be adapted for every kind of experiment. To provide a constant source of buffer solution and chemicals to be tested, we also need a fluid delivery system. Such a system will draw either the buffer solution or the solution to be tested from dedicated reservoirs and will inject them inside the microfluidic device in a temporally controlled manner.

To calibrate the optical setup and to run the first tests to confirm its ability to collect signals from calcium indicators, we employed a

20-fold magnification objective, injection pumps and a self-fabricated copy of the pulse arena described in [33]. For these tests, we focused on the visualization of calcium traces in the AWC^{ON} neuron. The AWC^{ON} neuron is either the left or right counterpart of the AWC neuronal class expressing the chemoreceptor gene str-2 [38] and senses 2-butanone and acetone [39, 40, 41]. The AWC^{OFF} neuron, does not express the str-2 gene but the srsx-3 gene and is sensitive to 2,3-pentanedione [39]. The AWC neurons have been reported to respond to benzaldehyde and isoamyl alcohol [42, 39] and to urine samples collected from cancer patients [15]. As odorant, we thus used a solution of 10^{-5} of isoamyl alcohol in a neutral buffer, namely SBasal (see section 5.8). Once the optical setup for calcium imaging was ready and calibrated (see section 5.2), we imagined the neural activity of target neurons in response to isoamyl alcohol under many different conditions: we tested different microfluidic chips to determine the best micro-environment to run chemosensation experiments in relation with parameter optimization of the fluid delivery system. We assessed the neuronal response reliability for many different stimulation patterns and for different isoamyl alcohol and urine concentrations as odorant solutions. We also determined the patient sample subset in which the response best fits the health condition of the subjects, which allowed us to define patient requirements for urine collections for such a test. The following subsections describe the strategy used to find the best conditions for experiments aimed at testing the response of *C. elegans* towards cancer metabolites in urine samples. The optimal set of protocols, materials and methods defined by the end of this preliminary phase of the work are discussed in section 5.

2.1 Chemotaxis assays and urine collection protocol

As reference values of accuracy in chemical sensing for comparison with calcium imaging experiments aimed at testing the *C. elegans* ability to detect cancer metabolites, we used previously available results of chemotaxis assays carried out with the joint lab Istituto Italiano di Tecnologia - Istituto Superiore di Sanità (IIT-ISS). Chemotaxis assays are broadly used in biology and allow to measure the

tendency of nematodes to migrate towards chemicals when placed at the center of petri dish. The result of such an assay is represented by a number, the so-called *chemotaxis index* (CI), ranging from -1 (complete repulsion) to 1 (complete attraction). In our case, to run a chemotactic assay, nematodes are placed on a 90 mm diameter petri dish divided in 4 equal sectors through straight lines passing through the center of the dish (see figure 6). Droplets of the chemical to be tested are placed on two specular sectors. The other two sectors contain droplets of a neutral chemical acting as a control substance. The region directly in contact with each droplet is previously soaked in sodium azide, which is able to anesthetize any nematode in the area, blocking them in place. One hour after placing the nematodes at the center of the petri dish, the chemotactic index can be calculated according to the following formula:

$$CI = \frac{N_+ - N_-}{N_+ + N_- + N_0,} \tag{1}$$

where N_+ refers to the number of nematodes found on the spot of the chemical to be tested, N_- refers to the number of nematodes close to the control droplet and N_0 refers to the number of any other nematode outside of the aforementioned regions. When the chemotaxis index is negative, the substance is perceived as repulsive, while a positive chemotaxis index is linked to attraction. These kinds of tests were used by Hirotsu and his team to prove the impressive ability of the N2 *C. elegans* strain to migrate towards urine samples of cancer patients. The results obtained with the joint lab IIT-ISS confirm the binary response of *C. elegans*: attraction when exposed to urine samples collected from women suffering from breast cancer at different stages, and repulsion when exposed to urine samples from healthy female subjects (with an accuracy of 86.11% measured over 36 breast cancer patients and 36 healthy donors). Further assays also proved that this behaviour belongs not only to the N2 strain, but also to two strains suited for calcium imaging: the PS6374 strain, which expresses calcium indicators in the AWC^{ON} neuron, and in the PS6364 strain, expressing calcium indicators in AWA neurons [42]. Both strains showed chemotaxis indexes towards isoamyl alcohol and benzaldehyde that were comparable with the ones obtained for the N2

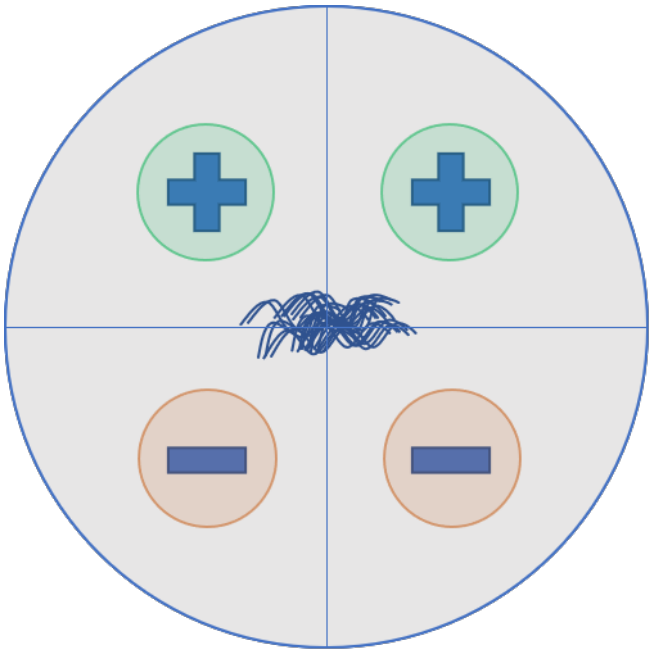

Figure 6: Outline of an agar plate (90 mm of diameter) prepared for chemotaxis assays. Nematodes are placed at the center, between four regions: two adjacent regions contain a droplet of the chemical to be tested (positive signs, green circles), while the other two contain a neutral substance acting as control (negative signs, red circles). The area covered by each droplet is previously soaked in sodium azide, so that after one hour, during which the nematodes freely explore the environment, any animal reaching these areas is anaesthetized on the spot. The chemotactic index is calculated according to the fraction of animals immobilized on each spot.

strain, meaning that chemotaxis is not altered by the presence of the calcium indicator.

Additional experiments showed how urine samples from female cancer patients undergoing chemotherapic treatment are invariably negative. The use of alcohol or cigarettes did not show significant alteration of the test: for the healthy subjects (3) who had stopped smoking for a week at the time they tested negative, the results did not change when going back to smoking. The same happened with

alcohol. Interestingly, the tests identified time-windows during the menstrual cycle related with a positive outcome of chemotactic assays: during the LH, FSH and estradiol release phase preceding ovulation, and during the progesterone peak in the luteal phase. Urine collected during these days or coming from patients taking drugs inducing the production of these hormones are incompatible with the tests. These results were used to identify the urine collecting protocol, defining specific requirements for patients and healthy donors providing samples to be tested in chemotactic assays and calcium imaging experiments. According to this protocol, samples are collected in the morning from healthy donors or female patients affected by breast cancer of any type (both lobular and ductal) at different stages. In the case of fertile women, samples need to be collected a few days after the end of the menstrual cycle or between its follicular and luteal phase. All samples analyzed in this work comply with these rules.

2.2 Different microfluidic devices

To run calcium imaging experiments while exposing *C. elegans* to urine samples in a systematic way, we use a microfluidic device. The microfluidic device is a PDMS chip that allows to confine nematodes in the field of view, in an environment that can be filled with liquid in a timely controlled manner. The first design that we tested was introduced in [33] and an example of its usage is described in [34]. It features inlet channels for buffer and odorant solutions, a nematode loading port and an outlet for liquid outflow (see figure 7). When loaded onto the chip, the nematodes flow into an arena covered in a forest of pillars that, besides supporting the chip structure, prevents the animals from assuming a closed loop posture, which impairs their ability to sense surrounding chemicals.

We used this design to produce many copies of the same microfluidic device. Each of the copy has been fabricated following the same, standardized procedure as the one described in section 5, but with a different set of parameters, including cooking time, plasma bonding time and power, and punching procedures. Although produced with

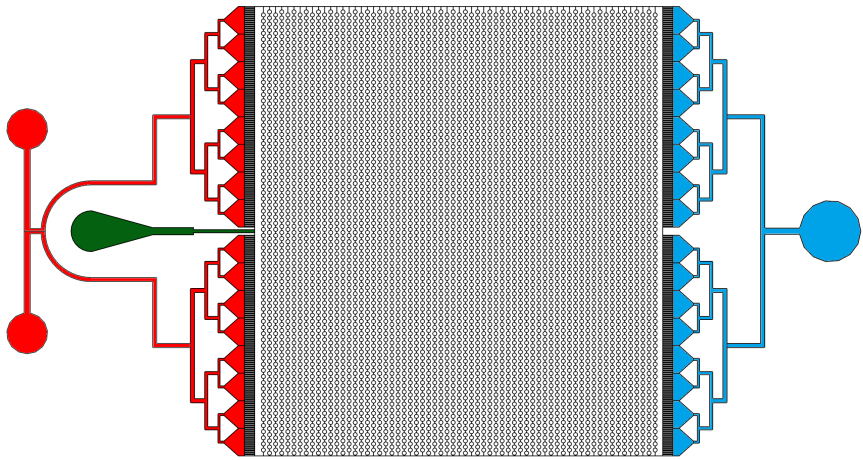

Figure 7: Design of the microfluidic device (outline of the Pulse arena by Albrecht et al. in [33]) for chemical pulses delivery. The chip features an internal arena with an area of 2×2 cm^2 and a depth of 70 µm). Buffer and odour inlets are on the left side coloured in red, while nematode loading port (100 µm $\times$ 1 mm channel) and outlet are coloured in green and blue respectively. The arena at the center features a forest of pillars and nematode barriers. The pillars are required to support the ceiling of the arena and to block the animals from assuming a closed loop posture, which would cover their noses preventing them from sensing surrounding chemicals. Their geometrical arrangement and their dimensions (100 µm of spacing in a hexagonal geometry with a diameter of 200 µm) have been defined in [33] as the best values to fit with the natural swimming movements of adult *C. elegans*. Worm barriers are 60 µm $\times$ 0.5 mm rectangular posts spaced 40 µm apart to prevent animals from leaving the arena while letting liquid through.

the same technique, each copy had different properties in terms of elasticity, sealing capabilities and operating pressure regime. After the preliminary tests, we verified that the pressure regime needed for these kinds of experiments is about 1.1 atm. Therefore, we resorted to an air plasma bonding at 600 mTorr of vacuum with a ratio of 1:10 of PDMS curing agent, which results in a device that is rigid enough

under such pressure, but also soft enough to absorb unintended high-pressure changes without producing any leakage.

To run the first experiments, we replicated this kind of arena and used it in conjunction with a 20-fold magnification objective to assess the response of chemosensory neurons with respect to different concentrations of isoamyl alcohol concentrations, a chemical that reportedly elicits attraction in *C. elegans*, and urine samples associated with a strong chemotactic index.

2.3 Different chemosensory neurons

From a connectionst point of view, the binary response of *C. elegans* upon chemical stimulation through urine samples is a downstream effect originating from the chemosensory perception of an odorant. It is reported that in *C. elegans* specific odors [42], and even specific concentration ranges [43], elicit a unique activation pattern of corresponding sensory neurons. In other words, some odors have a sort of signature in the temporal activation pattern of sensory neurons. This information, generated through sensing, is then processed through interneurons, which send signals to either avoid or approach the odour source, through the corresponding activation of motor neurons. However, when the information about the presence of a specific odour goes through these computational steps, it is weighed against other contingent stimuli that may affect the resulting behaviour, potentially altering the measured chemotaxis index (which is the only quantity used to determine whether the nematode has sensed aversive/attractive stimuli in the case of chemotaxis assays). The fact that the chemotaxis index is affected by the downstream activity of *C. elegans* makes chemotaxis assays very sensitive to contingent stimuli, requiring a high degree of control on the environment surrounding the nematodes.

Calcium imaging of the involved sensory neurons offers a way to indirectly measure the activation pattern upstream of the information flow. By providing a chemosensory stimulus in an otherwise stimulus-free environment, we expect to stimulate olfactory neurons in an odor-specific way. Therefore, by monitoring neuronal activa-

tion patterns in these conditions, we can assess whether the stimulus we provided is perceived as aversive or attractive, independently from the downstream behaviour. This is the reason why we chose to run these kinds of tests, expecting to reach a higher accuracy in predicting the attraction of *C. elegans* in response to urine samples.

C. elegans has a total of 30 chemosensory neurons clustered in either the head (25 cells) or in the tail (5 cells), see figures 2 and 3 as a reference. However, the only ones that reportedly mediate attraction towards urine samples coming from cancer patients are only 4 (see [15]): the AWA and the AWC pairs of neurons (see figure 8) right panels, both reported to sense attraction towards volatile attractants ([44] and [13]). Two other neurons are good candidates for mediating the avoidance behaviour from urine samples collected from healthy subjects: the ASH (a polymodal neuron) and the AWB neuron pair (for volatile molecules sensing), which are both reportedly associated with aversive stimuli ([13]).

To understand which neurons are mainly responsible for chemotaxis towards urine samples, we used the microfluidic chip described in section 2.2 and tested the response of the aforementioned neurons to chemicals associated with either a strong negative chemotaxis index (for neurons sensing aversive stimuli) or a strong positive chemotaxis index (for neurons sensing attractants). As reference for strong repulsion while assessing the response of the AWB and ASH neurons, we used a urine sample that tested negative multiple times in chemotaxis assays. As reference for attraction for the AWC and the AWA neurons, we used a urine sample that tested positive multiple times. It is worth to notice that the AWC neurons are reported to be odour-OFF neurons, meaning that they activate upon removal of the odour they sense and inhibited in its presence ([40]). Figure 9 shows typical responses from three of the four candidate neurons. The curve relative to the AWA neuron is not reported because of its low fluorescence signals, whose variations are difficult to measure. This neuron expresses a lower number of chemoreceptors if compared to the other attraction-mediating neuron (the AWC neuron), making it sensitive to a lower array of chemicals (see [12] and table 1). We therefore expect the AWC neuron to play a more significant

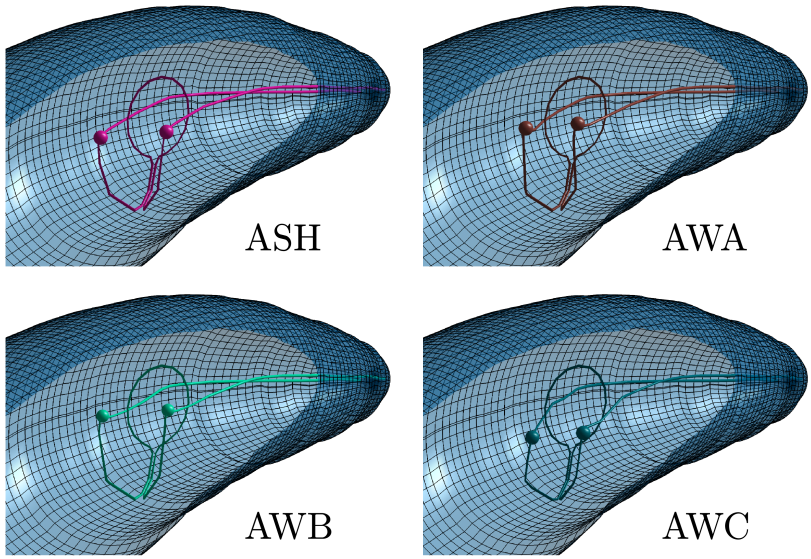

Figure 8: Chemosensory neurons mediating aversive response (ASH and AWB, left panels) and attraction (AWA and AWC, right panels) located in the head of *C. elegans*. All neurons present processes that extend to the tip of the nose.

role in mediating attraction. Chemotaxis assays carried out with the joint lab IIT-ISS confirm this hypothesis, showing how the genetic ablation of the AWC neuron (PY7502 *C. elegans* strain) is associated with a significantly abolished chemotactic behaviour towards urine samples collected from cancer patients. This suggests that we can discard the AWA pair as a first approximation in evaluating the attractive power of chemicals. Responses from the AWB neurons seem to not correlate with either addition or removal of attractant or repellent (although showing a calcium related dynamics during the experiment), while the ASH neuron does not exclusively respond to either attractant or repellent removal/addition. The AWC^{ON} neuron instead, already reported to respond to isoamyl alcohol, shows robust hyperpolarization during addition of attractant and strong depolarization

upon its removal in a stereotyped fashion.

Together, these results suggest that the best option for high-throughput experiments is to focus on the AWC^{ON} neuron, which produces reliable responses and strong fluorescent signals upon removal of positive urine samples. However, because this neuron is associated with attraction, it cannot account for repulsion sensed by the nematodes. To measure the overall tendency of *C. elegans* to respond through the activation of the AWC^{ON} neuron upon subtraction of a specific chemical, we can use the following quantity, which we call the neuronal activation index (NAI):

$$NAI = 2\left(\frac{N_{act}}{N_{tot}} - 1/2\right), \tag{2}$$

where N_{act} is the number of nematodes responding with the activation of the AWC^{ON} neuron and N_{tot} is the number of viable nematodes tested during the experiment ($\frac{N_{act}}{N_{tot}}$ is thus the activation rate). The subtraction of $1/2$ forces symmetry around zero, while the prefactor 2 grants that $|NAI| \leq 1$, projecting the quantity into the same range of the CI (namely $[-1, 1]$). From its definition, it follows that when $NAI > 0$, the majority of the considered nematodes experienced AWC^{ON} activation, while a negative value is associated with an activation in the minority of them. Additionally, if we assume that nearly all nematodes contributing to a positive chemotaxis index experience neuronal activation of AWC^{ON}, the N_+ appearing in eq. (1) corresponds to N_{act}, up to some background noise. This allows to create a relation between the two quantities, which may be useful for a comparison between them. Unfortunately, there is no counterpart in eq. (2) to account for nematodes that were repelled (N_-) during chemotaxis assays. To compare the two indexes, we thus need a scaling correction. The following formula identifies the correct relation between the NAI and the chemotaxis index (CI):

$$CI = NAI - \frac{N_-}{N_+ + N_- + N_0}, \tag{3}$$

where we also assume that N_{tot} appearing in eq. (2) corresponds to the sum of N_+, N_- and N_0, which have the same meaning as in eq.

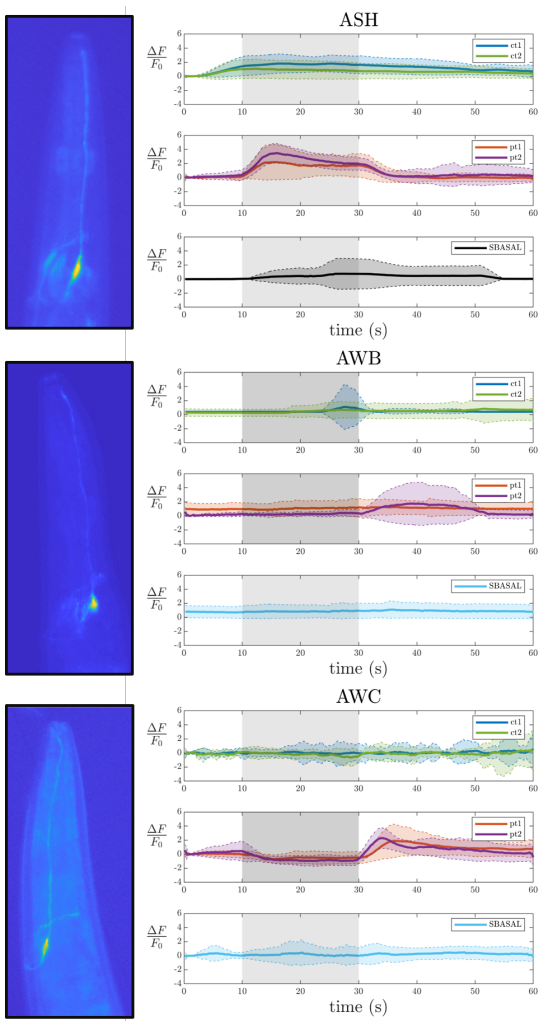

Figure 9: Mean percentage variation, $\frac{\Delta F}{F_0}$, of calcium imaging traces (see section 5) normalized according to standard deviation ($N = 6$) from (top to bottom) ASH, AWB and AWC neurons responding to control samples (repulsive), cancer patients urine samples (attractive) and to SBasal (neutral). Stimulus period is shaded in grey. ASH neurons respond to pressure changes related to flow switch, although showing a stimulus dependent activity. Traces from the AWB neurons do not seem to be reliable enough to explain the measured chemotaxis indexes. AWC^{ON} neurons show reliable responses, which make them the best candidate for comparisons with the CI.

(1) of section 2.1. From the equation, it follows that the *NAI* is an upper limit of the *CI*: if repulsion is neglectable in a specific process, $N_{-} = 0$ and the two indexes are equal, while $NAI > CI$ otherwise. With the relation described in 3, we can measure the consistence between the neuronal activation index and the chemotaxis index. It is worth to notice that we expect the *NAI* to be a better measurement of the tendency of a substance to attract/repel nematodes in absence of other stimuli: while it cannot directly match with the *CI* mathematically, it is expected to yield a higher contrast between the values associated with the group of healthy subjects and the values associated with the group of cancer patients, because it is dependent from an upstream measurement of the neuronal activity and not from a downstream output.

2.4 Sensitivity as a function of odorant concentration

The first tests to assess the sensitivity of the AWC^{ON} chemosensory responses were carried out using isoamyl alcohol concentrations. Isoamyl alcohol is reported as an attractive chemical for *C. elegans* eliciting the activation of the AWC^{ON} neuron upon its removal in a highly reliable fashion [42]. We exploited these responses to run tests aimed at setting many experimental parameters (like intensity of illumination, liquid injection pressure and camera exposure time) and to optimize the data acquisition process. After setting experimental parameters and external conditions, we tested concentrations ranging from a value of 10^{-6} to a value of 10^{-1}. The resulting response rates are reported in figure 10. The best range appears to be around 10^{-5}. However, this range may not be suited for experiments with urine samples, containing many different metabolites.

To identify the range of dilution that maximizes the sensitivity of the nematodes towards cancer metabolites, we focused on a subset of samples with a high index in chemotactic assays and that robustly elicits the activation of the AWC neuron in calcium imaging experiments at a concentration of 10^{-5} (which produced the highest response rates to isoamyl alcohol). From the same tests as the ones carried out for isoamyl alcohol (see figure 11), we found that the con-

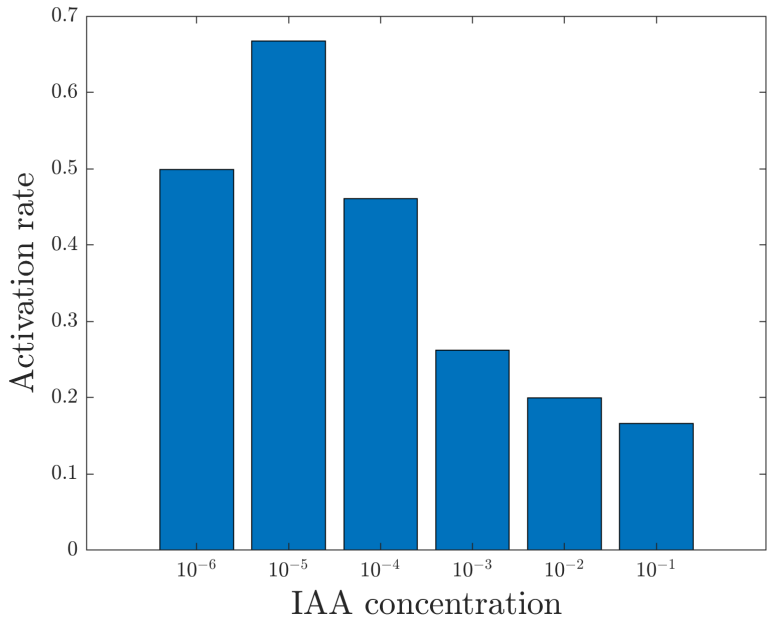

Figure 10: Activation rate (obtained as $\frac{N_{act}}{N_{tot}}$, see eq. 2) of *C. elegans* AWC^{ON} neurons in response to removal of isoamyl alcohol (y-axis) for solutions with rising concentrations (from 10^{-6} to 10^{-1}).

centration value that maximized the activation rate upon removal of urine samples from cancer patients is 10^{-2} (83.33% of activation rate for positive samples). At this value, the contrast between the activation rates, *AR*, of positive (pt) and control (ct) samples, $\frac{AR_{pt}-AR_{ct}}{AR_{pt}+AR_{ct}}$, is also the best one for the considered range.

2.5 Optimization for high-throughput experiments

To reach statistical significance in models subject to a relevant variability as the human one, we aimed at acquiring results for 36 patients and 36 healthy subjects. Each one of these urine samples needs to be tested in at least two different sessions, in which a minimum of 25 worms needs to be exposed to the odorant. This means that under the best conditions, defined in the previous subsections, we need to

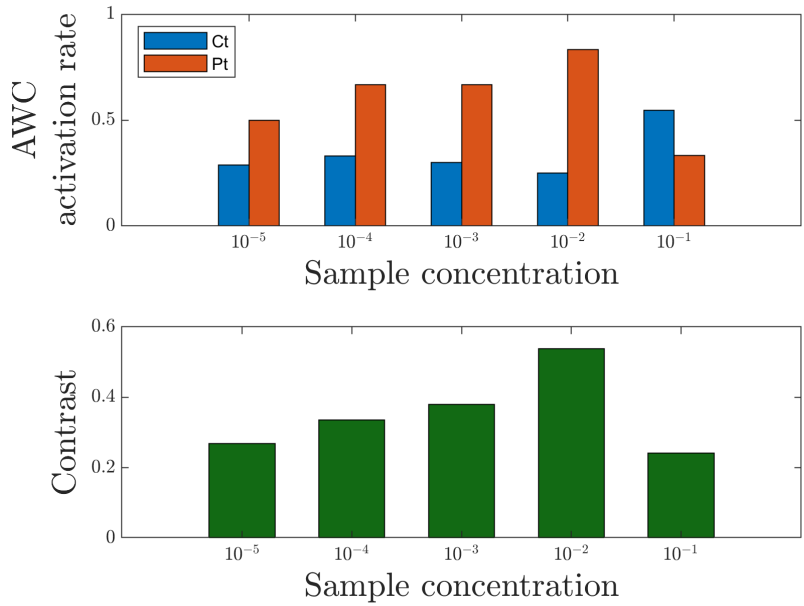

Figure 11: The top graph reports the activation rate of *C. elegans* AWC^{ON} neurons in response to removal of urine samples from cancer patients (y-axis) or control samples for solutions with rising concentrations (from 10^{-5} to 10^{-1}). The bottom graph shows the resulting contrast ($\frac{AR_{pt}-AR_{ct}}{AR_{pt}+AR_{ct}}$) for each concentration. Concentration of 10^{-2} yields the highest activation rate (83.33%) and the highest contrast between control and positive samples.

assess the response of single nematodes at least 3500 times. To limit the experimental time required by such a high number of tests, we decided to design a setup that is suited for high-throughput experiments employing a 4-fold magnification to simultaneously record multiple responses (see section 5 and 5.2). Additionally, to constrain the nematodes in the field of view of the 4-fold objective, we designed a custom microfluidic device (see section 5.3 and figure 25), which is a miniaturized version of the pulse arena described in section 2.2 (see figure 7). This is the final version of the setup used to obtain the results of this work, allowing us to simultaneously record calcium

traces from up to 25 worms in each acquisition.

With the final version of the setup, we tested different kinds of temporal patterns for the chemical stimulation. The temporal pattern parameters that may affect the *C. elegans* response during the experiments include the number of times the population can be chemically stimulated before it shows habituation, the time delay between consecutive stimuli, stimulation time and the amount of time they can stay in the microfluidic environment before showing stress-altered responses. By varying these elements around reference quantities used in reported experiments [34], we identified the best parameters set to reliably assess the nematodes response multiple times. Figure 12 shows AWC^{ON} responses to different example stimulation patterns. In these experiments, the reliability of the neuronal activation itself (neglecting its intensity) shows little to no dependence on recurrent stimulus presentation (as already reported in [45]), while the maximum amount of time granting clear and unbleached signals throughout the experiments seems to be of 2/2.5 hours per run. The choice of the stimulation time plays an important role in the outcome of positive samples testing, but not a pivotal one. This is due to the fact that the AWC^{ON} neuron responds in the form of graded potentials as opposed to all-or-none depolarization events. This means that there is no activation threshold to elicit changes in the signal collected from the neuron. However, if the stimulation time is too short, the chemical might not spread well inside the arena, and responses start to be more probabilistic and less deterministic, or too low to be detected.

In contrast to what happens with positive samples, the *NAI* associated with control ones shows a dependence on the stimulation time. Figure 13 shows AWC activation rates (top graph) and corresponding *NAI*s (bottom graph) obtained for the same control sample at the same dilution of 10^{-2}, presented for 10, 20, 30, 40, 50 and 60 seconds. As the *NAI* clearly shows, for stimulus exposure times of 40 seconds and more, the majority of the tested nematodes shows attractive-like responses, whereas shorter time-windows are associated with no response from most of the collected AWC traces. Considerations about this phenomenon in relation with the previously mentioned one are is discussed in section 4.

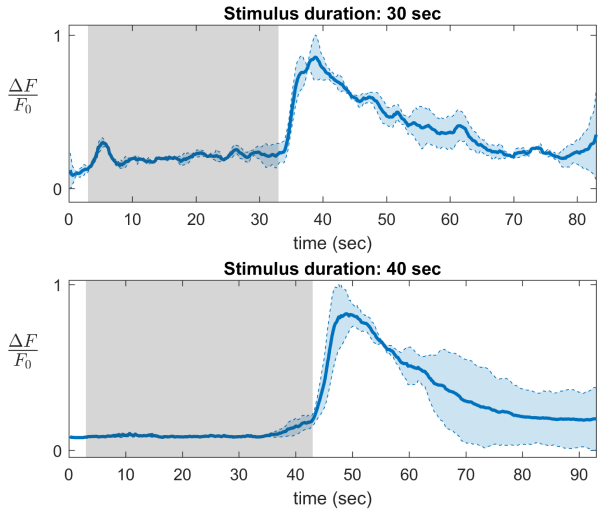

Figure 12: Two example experimental setups defining the temporal profile of the chemical stimulation pattern (gray shaded area), and the elicited AWC^{ON} min-max normalized responses (the blue line is the mean, blue shaded area indicates the range within one standard deviation from the mean): in both cases, there is a significant difference between the on-stimulus and post-stimulus activity. Noise is more visible in the curve following a shorter stimulation window, a result that is consistent with the analog nature of the responses of *C. elegans* neurons. It is worth to notice the small activity change visible right after the first liquid switch.

Therefore, to be sure to fill the entire arena and to detect significant changes in the recorded fluorescence, we chose to chemically stimulate for 20 seconds. As expected, if the time delay between consecutive stimuli is too short, calcium signals might be altered while ongoing. However, considering the aforementioned experimental time limit, a too long interstimulus interval would result in a lower number of tested samples per experimental run, in addition to

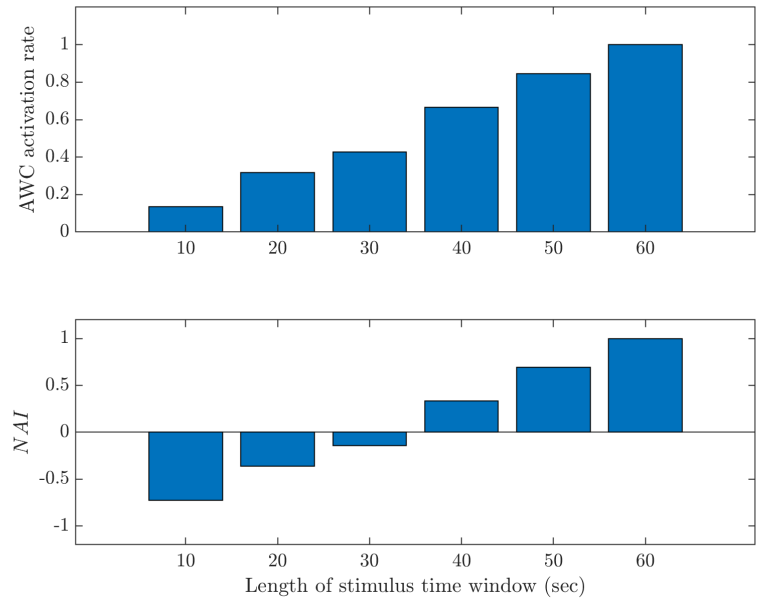

Figure 13: AWC activation rates and corresponding *NAI*s obtained for the same control sample as a function of the length of the stimulus time (top graph and bottom graph respectively). The *NAI* highlights how the stimulus presented for 40 seconds or longer times elicits attractive-like responses in the majority of the tested nematodes, whereas shorter time-windows are associated with no response from most of the collected AWC traces.

bigger data sizes, which are more difficult to handle. Therefore, we record for 30 seconds after stimulus removal and wait for a minute before starting a new test, granting at least one minute and a half of stimulus-free environment in the arena between consecutive tests. This set of parameters allows the AWC^{ON} neuron to reach its baseline fluorescence within acquisition time while avoiding responses from control samples. As an additional precaution, we chose to wait 3 minutes before testing a new sample. Whenever the stimulus is not injected, the buffer solution fills the entire arena, cleaning it from any chemical residues. It is worth to notice that the curves we obtained

often showed a small response to valve switching, which produces pressure and shear stress on the nematode (see section 6). Because of this, our experiments are always preceded by SBasal response tests, needed as a reference to exclude low amplitude responses from neu-

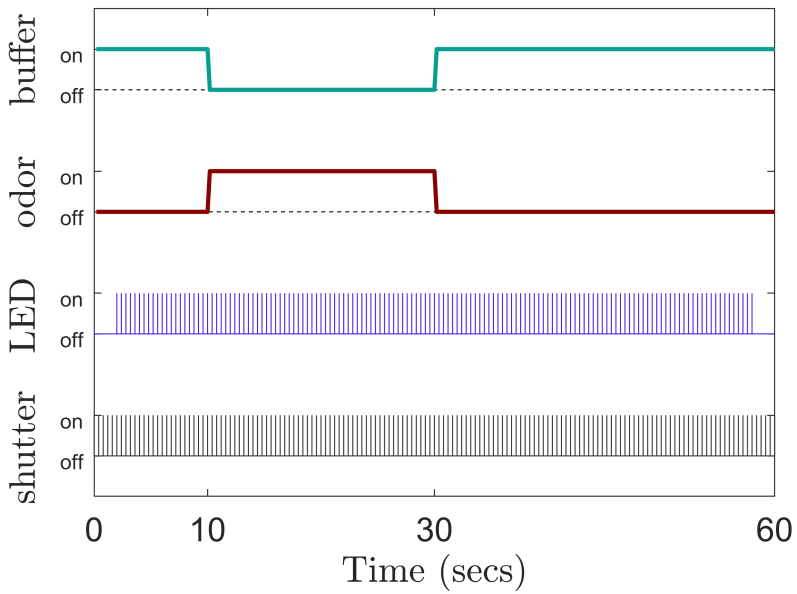

Figure 14: This is the temporal action sequence defined for high-throughput experiments that is passed to the device controlling the opening of the valves regulating the injection of odorant and SBasal, the camera shutter, and the excitation LED up to the tenth of a second. When the valves are on, the corresponding liquid flows into the arena. During the acquisition, buffer flows for the first 10 and last 30 seconds, while odour flows between these time-windows for 20 seconds. As shown in the figure, liquid switches occur at the 10th and 30th second of the test. The shutter of the camera is set to open and stay like this for 100 ms every 200 ms. The excitation LED activates in sync with the camera shutter after the first ten acquisitions until the tenth acquisition from the last one, shining for 100 ms every 200 ms. The first and last ten frames are used as a reference for background noise.

rons. Because of the definition of the *NAI*, SBasal responses are associated with repulsion/no response.

Figure 14 shows the final version of the temporal action sequence passed to the device controlling the injection of buffer, odorant, and the activation of the excitation LED and the acquisition device to the tenth of a second.

3 Results

After defining the best conditions to run high-throughput experiments, as described in the previous section, we started assessing the neuronal activation index (*NAI*, see section 2.3). We selected two groups of people: the first group includes 36 female patients affected by breast cancer of both types (lobular and ductal) at different stages from the first to the fourth; the second group is a control group of 36 putatively healthy women. None of the tested subjects had been taking drugs that may alter the hormonal cycle at the time of urine sample collection. For both groups, samples were collected following the urine collection protocol described in section 2.1. A description of each tested group is reported in table 2.

Each sample has been tested at least twice, in two different days of experimental runs, and the corresponding chemical solution was prepared using different stocked aliquots. Additionally, the response for each sample was tested in at least 25 worms for each experimental run. This means that the *NAI* reported for every patient is obtained considering a minimum of 50 nematodes. Figure 15 shows typical traces obtained with the protocols described in the previous section for one sample of both groups.

To calculate the *NAI*, we need to define a rule for the systematic identification of significant activation events in the AWC^{ON} neuron. To do this, we employ a custom script that extracts the fluorescence traces from the videos and evaluates them. Figure 16 shows the pipeline of the post-processing process for example images. The script proceeds as follows. After selecting the ROIs in a frame containing nematode heads (step 1 and 2), it applies a series of filters to clean the image and identifies the neuron (step 3 - segmentation). Once the neuron is identified, the script tracks it from frame to frame and constructs the fluorescence intensity curve in time, I, as $I = \frac{\Delta F}{F_0}$, where F_0 is the mean intensity in the first 10 seconds of the recording. In case significant motion is detected, the script discards the trace, as the signal might be altered by movement (step 4). When a viable signal is detected, it gets evaluated as according to the following rule (step 5): if the difference between the mean signal intensity in a 10

Classification			Type	
			Lobular	**Ductal**
	Primary tumor	**T und**	2 (5.6%)	0
		Tis	1 (2.8%)	0
		T0	2 (5.6%)	0
		T1	19 (52.8%)	4 (11.1%)
		T2	6 (16.7%)	0
		T3	0	0
		T4	2 (5.6%)	0
	Nodes	**N und**	1 (2.8%)	0
		N0	22 (61.1%)	4 (11.1%)
		N1	5 (13.9%)	0
		N2	4 (11.1%)	0
	Met.	**M und**	1 (2.8%)	0
		M0	30 (83.3%)	4 (11.1%)
		M1	1 (2.8%)	0
Total number			32 (88.9%)	4 (11.1%)

Stage	
Und	3 (8.3%)
0	2 (5.6%)
I	22 (61.1%)
II	0
IIIa	4 (11.1%)
IIIb	1 (2.8%)
IIIc	3 (8.3%)
IV	1 (2.8%)

Table 2: Number (and percentage) of positive samples for each classification characteristic and type of cancer on the left, and for each stage according to the AJCC/UICC staging system on the right. Notice that each percentage in a cell refers to the total amount of available samples (36) for the corresponding type of cancer. T refers to the primary tumor (original tumor), while N describes involvement of regional lymph nodes and M indicates whether or not distant metastases were found. "Und" stands for undetermined, while "is" for *in situ*.

second-long post-stimulus time-window, I_{off}, and the mean signal intensity in a 10 second-long time-window while on stimulus, I_{on}, is three times higher than the standard deviation of the signal in the time-window while on stimulus, σ_{on}, the response is associated with attraction. It is associated with either no response or repulsion otherwise. Using a comparison based on the standard deviation allows to detect significant calcium-related fluorescence changes independently from the absolute intensity of the signal, allowing to exclude low amplitude responses. However, the curves passing this require-

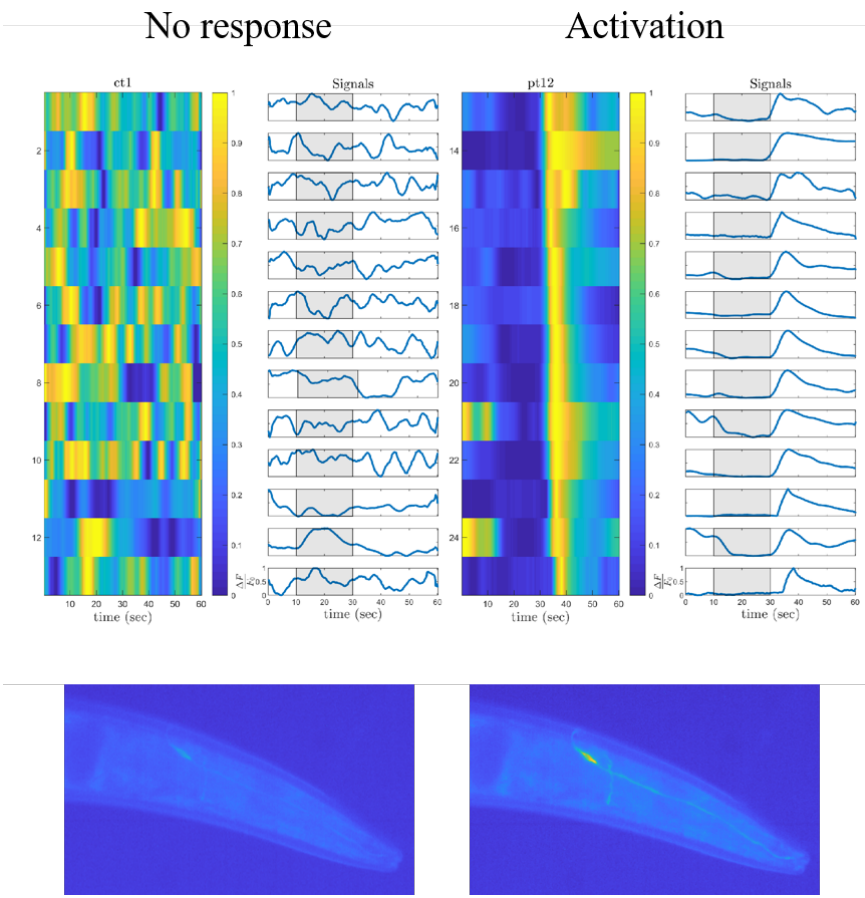

Figure 15: Heatmaps produced by typical traces recorded from the AWC neuron exposed to urine samples from healthy donors (on the left) and from cancer patients (right). Next to each heatmap the corresponding min-max normalized $\frac{\Delta F}{F_0}$ curves are reported. The two pictures at the bottom of the figure show an example frame of a head with a quiescent AWC^{ON} neuron (left) and a chemically stimulated one (right).

ment are then visually checked for consistence with the expected attractive response of the neuron (see section 2.4). Based on this expected response, we set the on-stimulus time-window of 10 seconds to start at second 12 of the recording, between the liquid switches of

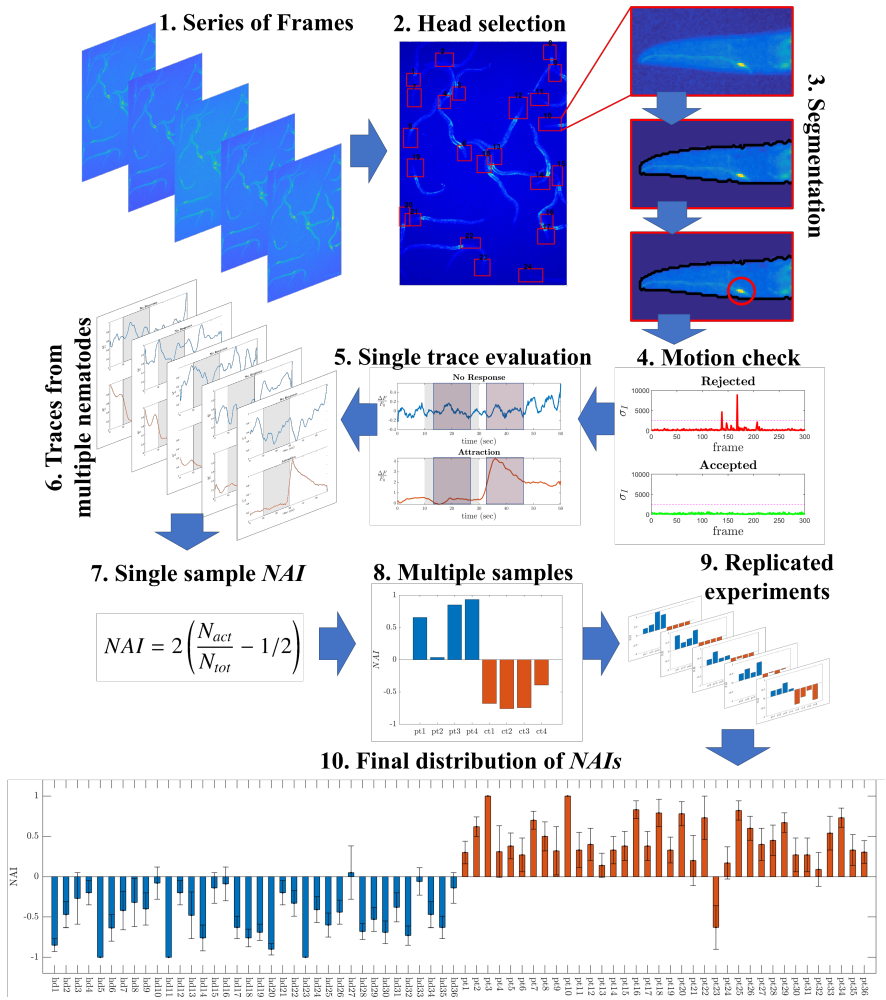

Figure 16: Scheme of the post-processing processes. Starting from a series of frames, heads are selected and segmented for AWC^{ON} identification. If the nematode is still during the acquisition, it will pass the motion check and the trace will be evaluated. The *NAI* is calculated considering all viable traces available in the acquisition. Each experimental run tests about 4 positive samples and 4 control ones. Averaging between different days of experiments finally yields an average *NAI* and a standard deviation for each sample.

the action sequence protocol (see Fig. 14), and a post-stimulus time-window of 10 seconds starting 2 seconds after the buffer substitutes the odorant. Because the activation of the AWC^{ON} neuron occurs upon attractant removal, this is a good way to understand whether the chemical tested is sensed as attractant or not. When all viable curves have been associated to either attraction or repulsion/no response (step 6), we calculate the resulting *NAI* for the tested sample (step 7). Therefore, at the end of the experiment we have *NAI*s for each tested chemical (step 8), and can integrate these results to previously obtained ones (step 9). In this way, we can evaluate a *NAI* considering all replicated experiments for each sample. The standard deviation to be associated with these values assumes a binomial distribution of the variables, and is calculated accordingly ($\sqrt{Np(1-p)}$, where N is the number of all nematodes assessed in all replicated experiments for a specific sample and p is the number of times in which the AWC^{ON} neuron activates upon removal of the sample.

The left graph of Figure 17 shows a bar plot reporting for each sample the resulting *NAI*, defined as in section 2.3, together with the corresponding standard deviation. Overall, there is a clear tendency in the *NAI*s obtained through calcium imaging: cancer patients are associated with a positive *NAI*, while healthy subjects have a negative *NAI*, meaning that the first group elicits the activation of the AWC^{ON} neuron as opposed to the second one, which does not trigger with the same frequency the chemical response in the neuron. There is one false positive (hd27) and a false negative (pt23), who does not show any significant difference with respect to the other patients in histological examinations or medical history. From chemotaxis assays carried out in triplicate through the joint lab IIT-ISS on the same set of samples, we produced a second bar plot, also reported in 17 (right). The measured *NAI*s are consistent with the results obtained in the chemotaxis assays, and with the assumption that the AWC^{ON} neuron mediates chemical attraction, contributing to a positive *CI*. However, the accuracy associated with calcium imaging experiments (97.22%) is significantly higher than the one obtained through chemotaxis (86.11%). The ROC curves as well, show how the *NAI* is associated with a better quantity to discriminate between

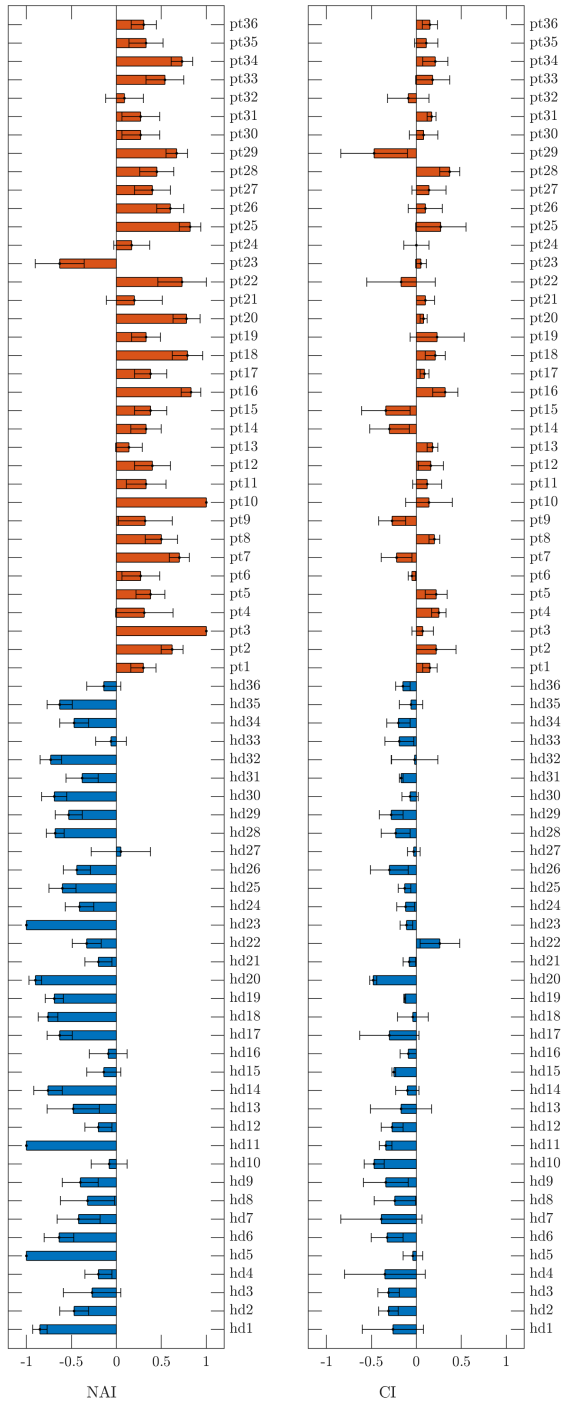

Figure 17: Bar plot of the resulting *NAI* (left graph) and *CI* (right graph) values for each sample of the control (blue bars) and positive group (red bars) reported with the corresponding standard deviation calculated assuming a binomial distribution of the variables. Although both indexes show a clear tendency (positive values for cancer patients, negative values for control group), the accuracy and the contrast associated with the *NAI* is evidently higher if compared to the *CI*.

the two groups of samples (see Figure 19, first two graphs on the left).

PCA analysis considering both indexes (reported in Figure 18) shows that the first component can explain 90.95% of the total variance. The *NAI* contributes to more than the 97.26% of the first component, highlighting its significance as discriminator. When looking at the distributions of the *CI*s, the *NAI*s and the first component of PCA (*PC*1), it is clear that the the last two values produce a better separation of the samples (see Figure 20). Interestingly, the accuracy associated with PCA1 is the same as the one obtained for calcium imaging, a surprising result considering that the *NAI* lacks a corresponding N_- term, accounting for repelled nematodes in the *CI*. This makes it more sensitive to detect attraction, while it is unable to distinguish between a lacking response and repulsion. In fact, the shape of the distribution of *NAI*s for control samples, which is more flat if compared to the corresponding distribution for positive samples, reflects this characteristic.

The higher accuracy of the *NAI* is consistent with the fact that the chemotaxis index is a quantity that depends not only on the ability of *C. elegans* to sense cancer metabolites in urine samples, but also on other contingent stimuli and events, which may mask the tendency of nematodes to move towards the tested chemicals. In fact, the chemotaxis index is a downstream result of a constant stream of a series of processes that include stimuli sensing, decision-making (based on the situation) and actuation. Any interference in any of these steps may inevitably alter the measurement of the chemotaxis index. On the contrary, the *NAI* is the indirect measurement of the activation of the AWC^{ON} neuron as soon as the chemical reaches the nematodes, upstream of the chemotactic process. There may be interfering elements in this kind of experiments as well (see section 6 for some examples), but if compared to chemotaxis assays (lasting one hour), the time-window in which these elements may alter the results is significantly lower, reducing the chances of this occurrence. Additionally, the use of a microfluidic device, designed to confine the animals in a controlled environment, further contributes to limit possible interference. To show how sensitive the *NAI* is compared to the *CI*, figure 21 shows for some of the samples a rescaled *CI*, *rCI*, that

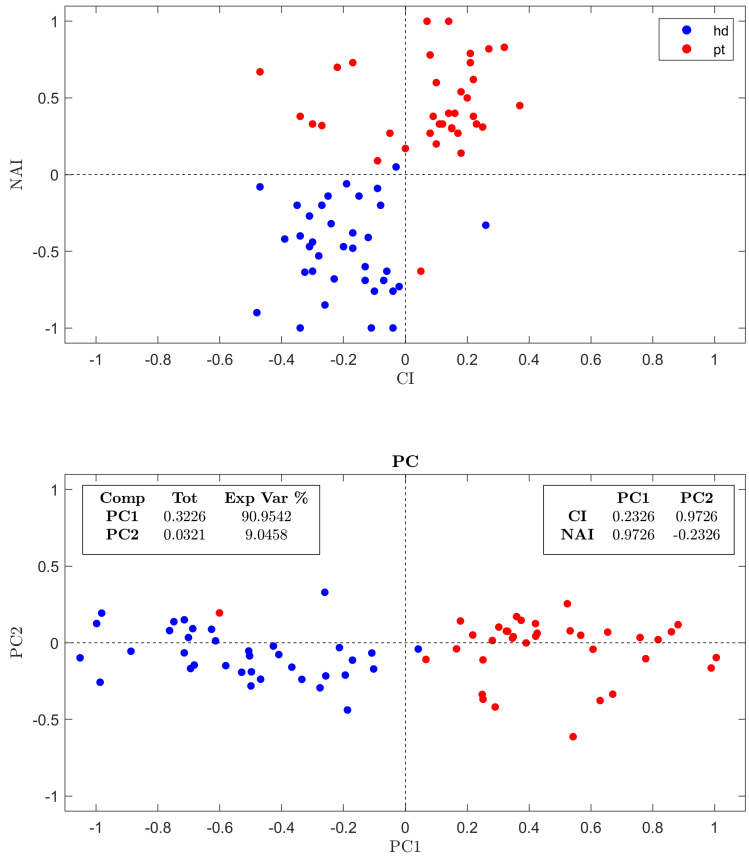

Figure 18: The top graph reports each sample in the plane *CI* vs. *NAI*. The bottom plot (PC1 vs. PC2) is the result of the PCA analysis of the top one. The text boxes report the outcome of the analysis, which show that the *NAI* values contribute to most of the separation between the points of the two groups.

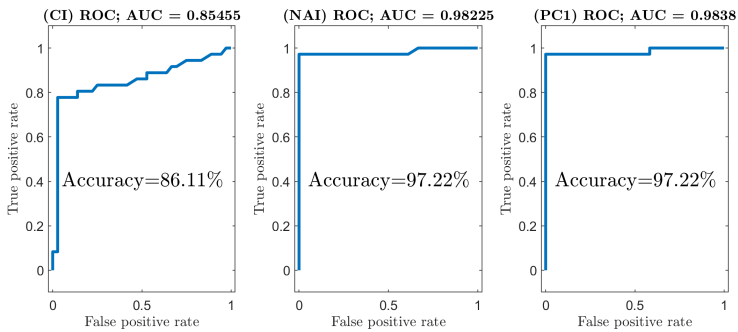

Figure 19: ROC curves obtained for the *CI* (left graph), for *NAI* (center graph) and the first component of the principal component analysis (right graph). It is clear from the graphs that the calcium imaging measurements yield a better discrimination between the positive group and the control one. Interestingly, the first component of the PCA does not improve the accuracy of the *NAI*.

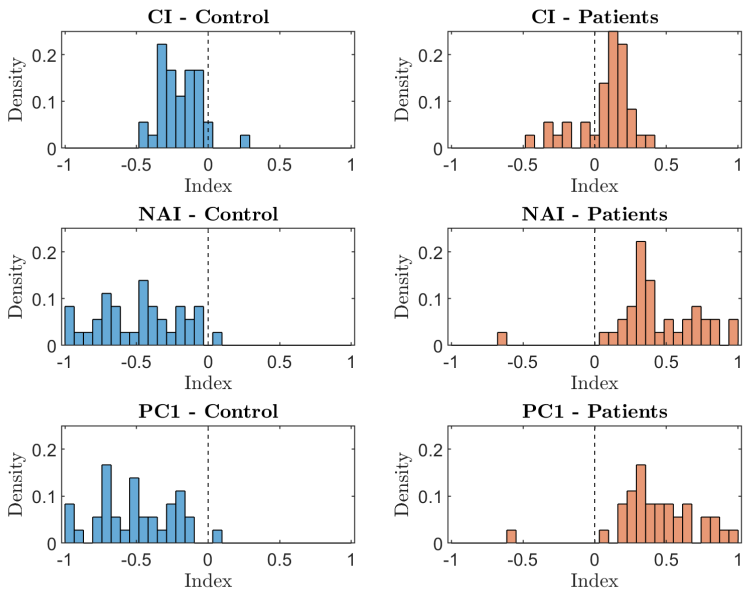

Figure 20: Distributions of the measured *CI*, *NAI* and *PC*1 (from top to bottom), for both the control group and patients (left and right graphs respectively for each row). The distribution in the second top graph on the left, with its flatter shape, reflects the inability of the *NAI* to distinguish between "no response" and "repulsion" when evaluating the nematodes preference with respect to control samples (which reportedly elicit repulsion).

would result if its calculation was based, like in the case of the *NAI*, only on the assessment of N_+ and N_{tot} (see equations 1, 2 and 3). The fact that *rCI* fails to correctly discriminate between the two groups suggests that its measurement is more subject to probabilistic factors (mainly concurrent stimuli and behavioural responses) and needs N_- as an additional constraint to reach a high accuracy.

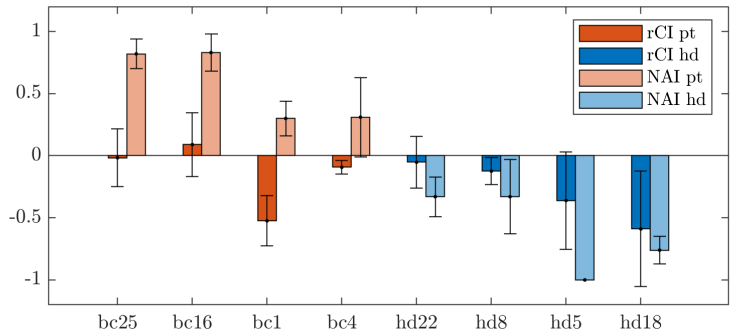

Figure 21: Bar plot showing for some of the tested samples the rescaled *CI*s, *rCI*s, that would result if their calculation was based, like in the case of the *NAI*, only on the assessment of N_+ and N_{tot}. The fact that *rCI* fails to correctly discriminate between the two groups suggests that its measurement is more subject to probabilistic factors (mainly concurrent stimuli and behavioural responses) and needs N_- as an additional constraint to reach a high accuracy.

The fact that the accuracy of the *NAI* evaluated only on the AWC^{ON} neuron is higher than the one associated with the chemotaxis index supports the hypothesis that this neuron plays the main role in mediating attraction towards urine samples. For this to be true, urine samples eliciting attraction must contain chemicals that interact with receptors on the membrane at the ciliated nerve endings of the neuron. This means that its receptors are good candidates as binding substrates for cancer related metabolites, providing chemo-physical constraints on the interacting metabolites. On the other hand, the high accuracy associated with the AWC^{ON} neuron also proves that chemical avoidance is not needed to discriminate between healthy samples and positive ones. However, *C. elegans* moves away from

negative samples instead of just not showing attraction towards them. This means that there is a concurrent mechanism contributing to the measured chemotaxis indexes, acting in a complementary way.

4 Discussion and conclusion

In this work, we built an optical setup and defined experimental protocols to assess responses of *C. elegans* neurons expressing calcium indicators while exposing them to timely controlled stimuli. We then applied this setup to assess the accuracy of *C. elegans* in discriminating between a group of women affected by breast cancer and a group of healthy donors. To do this we first ran a series of preliminary test that defined the experimental parameters and protocols to run high-throughput experiments and then tested the response of the AWC^{ON} neurons to removal of urine samples collected from both groups. The results obtained prove the impressive accuracy of the AWC^{ON} neuron to respond with activation upon removal of samples collected from patients affected by breast cancer of both lobular and ductal forms, at different stages. This ability can be quantified by a variable that measures the activation rate of the neuron in response to the stimulus, the neuronal activation index or NAI. The accuracy associated with the NAI is of 97.22%, which stays the same also when considered in conjunction with the chemotaxis index, CI, through the linear combination defined by the first component of a PCA applied to the plane (NAI, CI).

One of the most interesting application of this ability is for detection of cancer metabolites in urine samples at a low cost and on a large scale. Breast cancer is the most diffused cancer in women worldwide and is increasingly affecting developing countries, where most of the identified cases are diagnosed at late stages [46]. In fact, early diagnosis is a crucial element of successful treatment in most situations. In this sense, this work represents a first step to build a proof of concept for a screening instrument that is able to evaluate the presence of breast-cancer-related metabolites in urine samples through calcium imaging recordings testing the response of multiple nematodes. Canine scent detection [18] has already been successfully applied even at early stages to breast cancer [19], colorectal cancer [20] and lung cancer, reported to be sensed by rodents as well [21]. However, the practical problems of dealing with mammals in hospitals or clinical facilities represent a huge drawback in the application of these kinds

of diagnosing options. On the contrary, the introduction of nematodes in such facilities does not represent a risk for patients, and their ease of cultivation makes it an affordable alternative to the currently available tests based on the identification of biomarkers [16], which do not reach the same accuracy as the one obtained in this work [17] and are often unfeasible on a large scale. In comparison to mammography or ultrasound based screenings, which allow to know the position, dimension and type of cancer, this test would be quicker, less bothersome for the patient and more affordable for national health systems, useful as a pre-screening evaluation.

As supported by our results, the advantage of exploiting the *NAI* in the design of an instrument for cancer detection with *C. elegans* is that its accuracy would be considerably higher if compared to chemotaxis assays. The higher specificity and sensitivity is linked to the fact that chemotaxis assays depend on downstream effects of decision making processes that are very sensitive to concurrent stimuli throughout the duration of the assay (like vibrations, temperature or the number of testing nematodes). This noise gives the *CI* a probabilistic component that reduces its associated discrimination power. Additionally, the testing time required for behavioural assays is much longer. On average, we could measure calcium traces of at least 25 nematodes for about 4-6 samples in 1 hour, which is the amount of time required for a chemotactic assay. The testing conditions (different time-windows, variation of concentration, temperature, pressure) did affect the response of the AWC^{ON} neuron, but the sign of the *NAI* is stable with respect to these changes. Considering the behavioural variability affecting the chemotaxis assays, this is an additional advantage of the *NAI* if compared to the *CI*. Interestingly, the lack of a signal representing repulsion in calcium imaging is not sufficient to make the *CI* more specific and/or more sensitive than the *NAI*. To this extent, it would be interesting to investigate the variability observed in the AWB responses (figure 9), to understand if they can be associated with a lack of response and/or repulsion. In any case, if we consider the potential applicability of the *NAI* as a screening parameter on a large scale and its high accuracy, having a higher probability of false positives and a lower probability of false negatives is prefer-

able than the opposite situation, which would result in a small chance of undiagnosed cases.

Taken together, these results represent an initial step in the definition of a cancer screening method, which need to be complemented with further experiments. The samples considered in this work include a group of 36 breast cancer patients and 36 putatively healthy women. The average age of the first group (67.1±12.2) are higher if compared to the second one (43.6±15.6) due to the incidence rate of the disease in the corresponding age ranges and to difficulty in collecting urine samples from older healthy donors. However, we saw that the *CI* as a function of menstrual cycle has a higher contrast in young women, suggesting that it would be of great help to collect samples from younger women affected by breast cancer, to see if the accuracy is affected by age. An other complementary test involves patients affected by pathologies that might produce similar metabolic traces in urine samples as the tested positive samples (inflammatory states like mastitis for instance). In this sense, we are obtaining promising results for urine samples associated with prostate cancer, sensed as attractants by the nematodes, and prostatitis, which do not elicit significant responses.

An other interesting conclusion related to the results is that they suggest a possible way to partially predict the shape and the chemophysical properties of the metabolites involved in breast cancer. To discriminate between the two groups, *C. elegans* must have receptors that allow it to sense a concentration difference between a set of metabolites contained in the urine samples it responds to. We assume that to do this, receptors on the AWC^{ON} neuron must bind with these metabolites. By studying the shape of the involved receptors (which may be identified trough calcium imaging tests on mutants), we can extract a set of expected chemo-physical properties of the involved metabolites. In fact, given the positive outcome of this work, this study will be followed by a chemical analysis exploiting gas chromatography–mass spectrometry carried out on a subset of the samples tested here. The analysis will be complemented with the prediction of the structure of chemoreceptors expressed by the AWC^{ON} neuron. This information will be used to predict binding affinities

between each metabolite associated with a significant concentration difference between positive and control samples and the involved receptors in *C. elegans*. Any metabolite presenting high binding affinities will be a putative biomarker for cancer. An other information that may help the identification of relevant chemicals is related to the fact that the ability of *C. elegans* to sense cancer metabolites is likely to rely on a similarity between chemicals produced by bacterial populations (the food source of nematodes) and metabolites produced by proliferating cells. As an example, a recent study [41] identified a set of odorants of bacterial origin that elicit attraction in *C. elegans*, which may add other hypothetical references for the chemo-physical properties of cancer related metabolites. It is also worth to notice that, chemosensation in *C. elegans* has been recently reported [47] to break the so-called "Independence of Irrelevant Alternatives" (IIA) logical rule [48]. This rule states that the presence of a third option should not affect the preference of a subject between two other options. According to what described in [47], different ratios of attractive and repulsive components of a mixture can activate asymmetrically the neuronal architecture involved in the sensation of odours resulting in the violation of this basic axiom of rationality. In other words, when sensing positive urine samples, *C. elegans* expresses a choice that may be dependent not only on the presence of a characteristic metabolic profile, but also on the concurrent chemical background. If this is true, the research of involved metabolites may become difficult, requiring to be extended to compounds that show partial to possibly no similarity to the chemicals that the AWC^{ON} is able to sense. To this extent, an additional information that may be taken into account when looking for candidates for biomarkers is the inversion of the *NAI* value at high concentrations (10^{-1}). The fact that control samples become attractive at those concentrations suggests that they contain attractive chemicals at a lower concentration if compared to positive ones. However, too high concentrations of these metabolites become repulsive as shown in figure 11. In line with this, also the results for different stimulation time-windows of control samples are instructive (figure 13). The inversion of the preference highlighted by the *NAI* also suggests that control samples contain chemicals that are

able to elicit a response in the AWC^{ON} neuron upon removal depending on the duration of the stimulus. Longer time-windows probably promote the chance of interacting with ligands sensed by the neuron.

As a side note, this study also offered the chance to detect an interesting secondary response of the AWC^{ON} neuron, probably elicited by shear stress produced by pressure changes. This kind of response is represented by a depolarization that is visibly less intense than the one associated with chemosensation, but still detectable in some of our recordings. It would be interesting to understand how two stimuli of such different nature may affect the activity of a neuron that is considered to be primarily chemosensory. Because this effect may also depend on internal activity of the chemosensory circuit and other neurons, it would be helpful to study calcium imaging traces of neighbouring neurons, to understand the origin of such a phenomenon. Pan-neuronal calcium imaging has already been successfully applied to the *C. elegans* nervous system [49, 50] even while freely roaming [51] or targeting the behaviour of the AWC neurons [52]. Including other neurons in our calcium imaging experiments would allow us to shed a light on the origin of the AWC response to pressure changes and its effect on chemosensation.

In conclusion, this work highlights the ability of *C. elegans* to sense metabolites in urine samples related to malignant growth, suggesting that this discrimination power may be exploited to help contrasting such a complicated disease as breast cancer. This may be achieved not only through the design of a screening tool for early diagnosis, which is of crucial importance for the considered pathology, but also to help identify the main metabolic pathways involved in the disease, in the hope that it will support the creation of new possible treatments.

5 Materials and Methods

To study the response of *C. elegans* to different odour stimuli we used a specific strain expressing calcium indicators in one odour responsive neuron (namely AWC^{ON}) and an optical setup that allows to record calcium dependent fluorescence. In this design, nematodes are confined in a custom designed microfluidic chip, which is placed on a moving stage above the objective of the optical setup and connected to the fluid delivery system. The fluid delivery system allows to fill with arbitrary solutions the microfluidic chip containing the nematodes, through a set of tubes, electrovalves and pressurized bottles in a temporally controlled manner. Each step of the experiment preparation and conclusion are defined by protocols reported in this section. The study was approved by the research ethics committee of "Fondazione Santa Lucia", Italy (see appendix B). Patients gave written consent to participate.

5.1 *C. elegans* strains

C. elegans strains were cultured at 20° C under standard conditions on NGM plates [53] using Escherichia coli OP50 as source of food. We used N2 animals as a wild type strain for behavioural assays, the PY7502 strain for experiments with AWC-ablated strains, available at the *Caenorhabditis* Genetics Center, Minneaplolis, MN, (genotype ceh-36p::TU813 + ceh-36p::TU814 + srtx-1p::GFP + unc-122p::DsRed), while for neuronal response assays, we used the PS6374 C. elegans strain (genotype pha-1(e2123ts); him-5 (e1490); syEx1240 [str-2 :: GCaMP3 + PHA-1]), a kind gift from the Zaslaver laboratories (The Hebrew University of Jerusalem, Jerusalem, Israel), studied in [42]. This strain expresses a calcium indicator (excitation at 485 nm, emission at 510 nm), namely GCaMP 3 [35] in the AWC^{ON} neuron, which responds to attractant removal [42].

5.2 Optical setup

The optical setup is shown in figure 22, and is made of the following elements (numbers in parenthesis refer to the outline shown in the figure):

- An optical table (stainless steel) supporting one breadboard (anodized aluminum);
- A CMOS camera for image recording (9)
- One pass-band filter at 3 cm in front of the camera to limit the frequency range of the recorded signals in a specific domain (8)
- One mirror at 7 cm in front of the pass-band filter to reflect the signal from the sample to the camera (7)
- One dichroic filter 5 cm above the mirror to reflect the excitation light onto the sample without affecting its emitted fluorescence path (6)
- One objective above the dichoric filter to gather the light from the sample at a varying distance depending on the objective type and the required focal plane distance (5)
- One x/y-moving stage above the objective supporting the microfluidic chip containing the sample (13)
- One blue LED (470 nm) for calcium indicator excitation shining its light from a distance of 7 cm onto the dichroic mirror and on the sample (10)
- One red LED (660 nm) for transmitted light visualization (1)
- One mirror in front of the red LED at a distance of 7 cm to reflect light on the sample for transmitted light visualization (3)
- Two condensers placed right in contact with each LED to make the light beams parallel (2 and 11)

- One excitation filter in front of the blue LED at a distance of 2 cm to restrict the emission frequencies in the desired range (470±10 nm), given the spectrum of LEDs, which is typically broad (12)

The red channel (λ=660 nm) is used for light transmission (sample is illuminated from above and observed from below), while the blue channel (λ=470 nm) excites the calcium indicator expressed in neurons allowing calcium imaging. This works in reflection (illumination and observation from below). The red LED (number 1 in figure 22) generates light with a Gaussian distribution of frequencies peaked at about 660 nm. Its emitted light travels through the condenser (number 2) which makes the beam parallel and reaches the mirror (number 3) which reflects it onto the sample (number 4). The light transmitted from the sample is then collected by the objective (number 5) and goes through the dichroic mirror (number 6) reaching the second mirror (number 7), which reflects it through the second filter (number 8) and finally to the camera (number 9). The blue LED (number 10), used for calcium indicator excitation, produces light with a Gaussian distribution of wavelengths peaked at about 470 nm. The light travels through the condenser, which makes the beam parallel (number 11), is filtered by the excitation filter (number 12) and reaches the dichroic mirror (number 6), which reflects it onto the sample (number 4). Calcium indicators inside selected neurons of a specific *C. elegans* strain absorb the incoming radiation and subsequently emit fluorescence light at 510 nm in a calcium dependent manner. Part of the signal emitted by calcium indicators is collected by the objective (number 5) and goes through the dichroic mirror reaching the second mirror (number 7) that reflects it through the second filter (number 8), which reduces the collection of green light letting other frequencies pass through reaching the camera (number 9).

Depending on the objective in use, this optical setup can operate at a 4-fold or 20-fold magnification level. The first one (4X objective with a numerical aperture of 0.28) allows to perform high-throughput experiments, with multiple nematodes in the field of view, while the second one (20X objective with a numerical aperture of 0.40) provides a better visualization of one single head. Each magnification

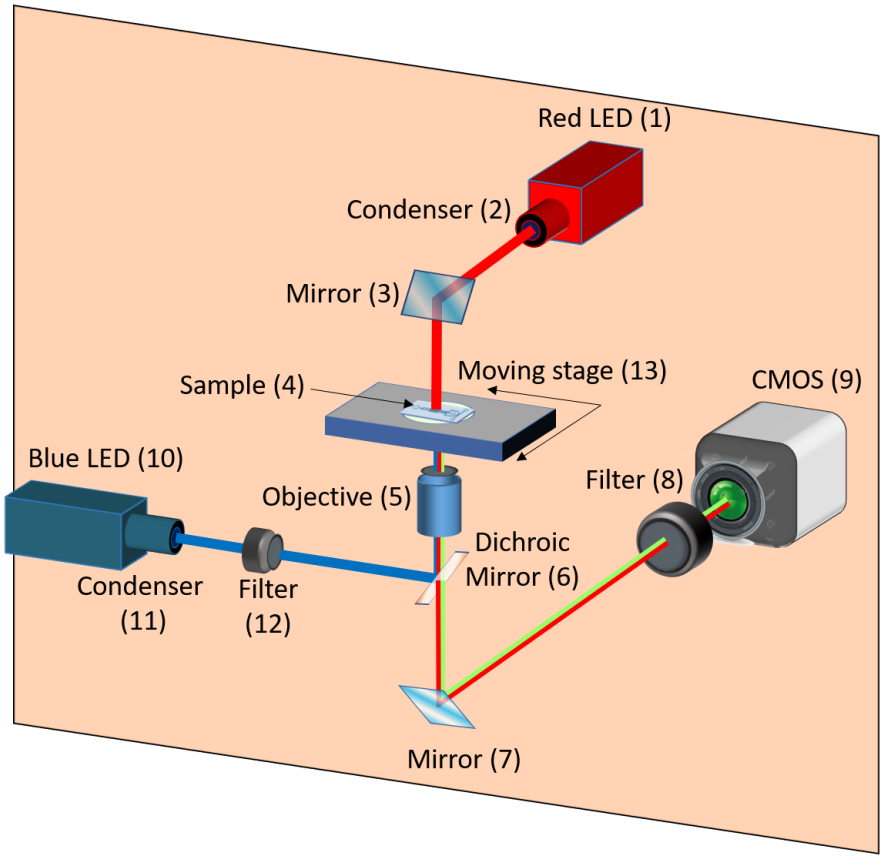

Figure 22: Outline of the optical setup. The red line highlights the optical path of the transmission channel used for *C. elegans* inspection and ROI selection. The light travels from the red LED (1) through a condenser (2) and gets reflected by a mirror (3) onto the sample (4), from which the transmitted light is collected through the objective (5), goes through the dichroic mirror (6) and is reflected by a second mirror (7), finally reaching the CMOS camera (9) through a second filter (8). The blue line represents the optical path of the excitation channel. After passing through a condenser (11) and a filter (12), the light generated by the blue LED (10) is reflected by the dichroic mirror (6) onto the sample (4), where it can excite calcium indicators, eliciting a calcium-dependent fluorescence. Part of the fluorescence is collected by the objective (5) and reflected by a mirror (7) onto the camera (9), passing though a filter (8).

has been validated through calibration with μm and nm rulers.

During a stereotypical test, the system is set to record images at a frequency of 5 Hz, with the shutter open for 100 ms. This parameter set allows to indirectly measure neuronal calcium dynamics avoiding the bleaching of the calcium indicator caused by continuous illumination. When the excitation light is in action, the blue LED activates in synchronization with the acquisition of the CMOS. The blue LED light power is analogically controlled and adjusted to a trade-off value, which needs to adapt to the overall *C. elegans* calcium indicator expression levels, taking into account that too high values can produce significant bleaching that may invalidate the test.

5.3 The microfluidic chip

To control the environment surrounding the nematodes during chemical response testing, we chose to confine the animals in a microfluidic device of custom design outlined in figure 23. The chip is made following the protocol described in section 5.4 and consists of a PDMS polymer bonded on a glass substrate.

Upon injection through either one of the two inlet ports, the liquid flows into two 275 μm wide channels that lead through worm barriers into an about 3×3 mm^2 arena. The arena is covered in a forest of pillars arranged in a hexagonal geometry that prevents the nematodes from assuming the closed loop posture, which can inhibit chemical sensing through their noses, without completely disrupting their movements. This is achieved with a pillar spacing (100 μm) adapted to the spatial frequency of *C. elegans* body bends and with a pillar diameter (200 μm) that is adapted to their bending amplitude. From the arena, the injected liquid flows through another worm barrier to the outlet port. The thickness of the chip is 50 μm. A loading port allows to load nematodes directly into the arena through a tampered 150 μm wide channel. The design is based on the pulse arena described in [33]. However, compared to the arena described by Albrecht and Bargmann, our device is smaller and has a denser worm barrier. These modifications allow it to confine up to 20 nematodes in the field of view of the microscope and limit the risk of flushing out

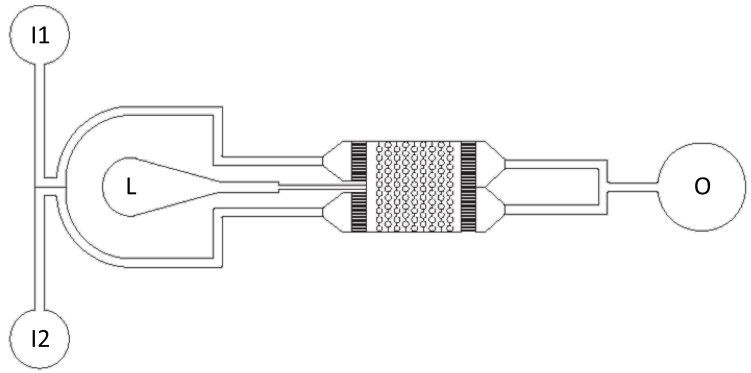

Figure 23: Mini Pulse Arena Outline. The flow is directed through 275 μm wide channels from either one of the two inlets (I1 and I2) through the arena (area: 3×3 mm^2) filled with pillars (pillar diameter: 200 μm; pillar spacing: 100 μm; arranged in a hexagonal geometry) towards the outlet (O). The loading port (L) allows to load nematodes into the arena and to deliver levamisole for paralyzing through a tampered channel (final width: 150 μm).

worms.

Before loading the nematodes onto the chip, the device needs to be completely filled with liquid, and remaining air bubbles, which can prevent the complete flow distribution inside the arena, need to be removed. To do this, we put the device in a plate filled with distilled water, and degas it for 30 minutes with a vacuum pump, until bubbles are completely gone. To connect it to the odorant delivery system, the Tygon^{TM} tubes of the system (with an inner radius of 0.020 in) are connected through canulae to the inlet ports of the chip. The connection has to occur with dripping cables and water-covered chip, to prevent any bubble formation inside the arena. Once the first connection is completed, the chip can be taken out from the plate with distilled water, and the following connections can be performed with a drop-to-drop technique (see figure 24): before attaching a cable to any port, the canula at the end of the cable needs to be dripping liquid and the port needs to be covered in liquid pushed out from the device, so that both endings are inaccessible to air. The connected chip is

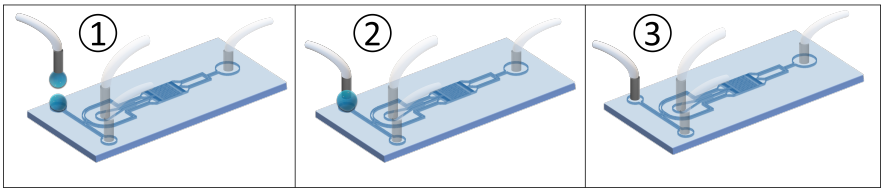

Figure 24: The drop-to-drop technique: to connect the Tygon^{TM} tube to the chip we first push out a drop of water from the tube and from the port (1). We then carefully insert the canula inside the drop of water making sure to keep it above the port (2). Once the canula is inside we gently push it through the port hole (3). This connecting procedure is important because it significantly lowers the chance of getting air inside the chip.

outlined in figure 25. Once the experiment is completed, the devices are sterilized with alcohol and bleach and then trashed.

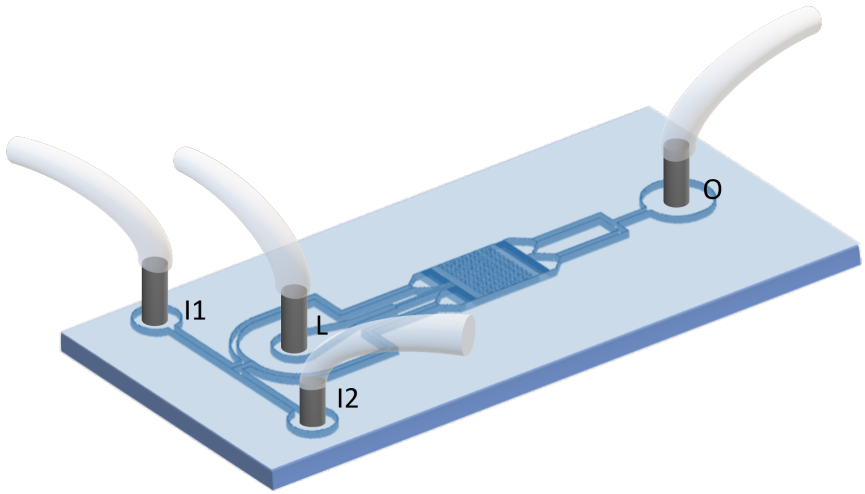

Figure 25: Mini Pulse Arena connected to the fluid delivery system. The buffer channel is connected to the I1 port, the odorant channel to the I2 port and the levamisole/nematode loading channel to the L port. An other tube is attached to the O port for liquid outflow. All connections are performed with the drop-to-drop technique to ensure no air enters the chip.

5.4 Microfluidic device fabrication

To produce the microfluidic chip we resort to soft lithography techniques [37]: we employ a mask to generate a mold used to replicate the chip using a Sylgard™ 184 PDMS polymer. The main step of the process are summarized in figure 26. We first design the chip in AutoCAD™ and then commission a high resolution film photomask to an external laboratory. Once the mask is available, we start the fabrication process by preparing the mask for soft lithography. We wash a glass cover with soap and water and then dry it with compressed air and a cloth suited for optical instruments. We then take the mask and put it on the glass cover taping its angles to keep it still and place the glass cover with the mask side facing downwards in the UV-exposure device. We leave the mask there and go on preparing the substrate for soft lithography, which will also go in the UV-exposure device. To prepare the glass substrate we first clean it with a Piranha solution and then wash it in distilled water and dry it with compressed air. To hydrogenate the glass, we put it in the oven at 180° C for half an hour and then on a hot plate at 65° C for 10 minutes. After coating it in a layer of SU-8 3050 negative photoresist, we spin it on a spin coater to obtain a thickness of 50 µm and heat it in 3 cycles on hot plate at 65° C for 2 minutes, at 95° C and then at 65° C for two minutes to avoid thermal shock. At this point, we put the glass substrate in the UV-exposure with the mold, and start the device. After photoexposure we heat the substrate again at 65° C for 2 minutes and at 95° C for 7 minutes. After some cooling time, we soak the glass substrate in the developer, which will remove the non-polymerized material, and use isopropyl alcohol to wash away the debris. After this step, we heat it for two minutes on the hot plate at 65° C and then for 30 minutes at 180° C. At this point the mold is ready and can be used multiple times to produce many microfluidic devices.

To fabricate the chips through the casting process, we mix about 10-15 g of Sylgard™ 184 PDMS per chip and mix it with the curing agent in a ratio of 1/10. Once the material is properly mixed and filled with bubbles we degas it, pour it on the mold, and degas it again. After baking the material on the hot plate at 80° C we let it rest for 1 hour and make the inlet ports, the outlet port and the loading

port using a 0.5 mm puncher. To finally bond the PDMS on a glass substrate, we employ an air plasma bonding device at high power for one minute.

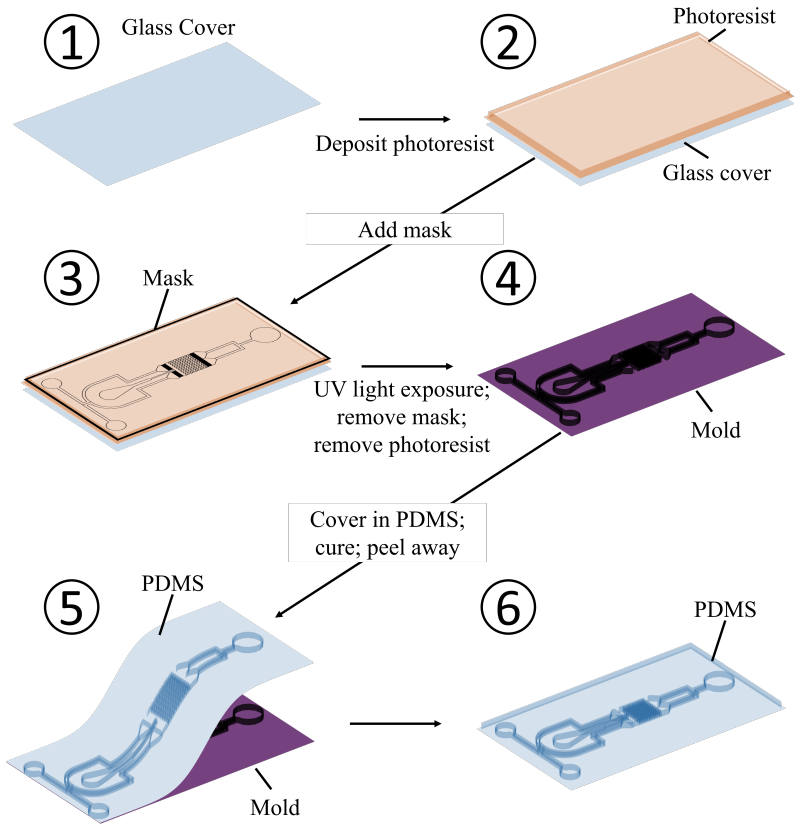

Figure 26: Summary of the main steps of soft-lithography. The process starts from a glass cover (1), which acts as substrate for the photoresist (2). Covered by the mask, they get exposed to UV light (3). This results in the creation of the mold (4). Every replica of the chip can then be produced by pouring PDMS on the mold, baking it and peeling it away (5 and 6).

5.5 Odorant delivery system

To test the chemical response of *C. elegans*, we used a fluid delivery system (outlined in figure 27) that can provide in the microfluidic device either a constant flow of buffer solution (SBasal) or a constant flow of a solution of choice. When the nematodes are loaded onto the chip and ready for testing, the device is attached to the fluid delivery system. This system consists of:

- A constant pressure source of 1.1 atm
- One pressurized bottle
- One pressurizing cap compatible with 5 ml falcons
- Two Tygon^{TM} tubes (dimensions: inner radius 0.020 in, outer radius 0.060 in, 30 cm long) for liquid collection from the pressurized bottle and the pressurizing cap
- A supply line with a T-junction (Tygon^{TM} tubes with 0.5 cm diameter), connecting the pressure source and the pressurized bottle and pressurizing cap.
- Two electrovalves to control liquid flow
- Two soft Tygon^{TM} lines passing through one electrovalve each
- Two separate Tygon^{TM} lines (dimensions: inner radius 0.020 in, outer radius 0.060 in) connecting respectively the pressurized bottle and the pressurized cap with the two separate lines of soft Tygon^{TM} tubes through plastic fittings.
- Two Tygon^{TM} lines attached through plastic fittings to the two soft tubes, connecting them to two metal canulae to be inserted in the inlets of the microfluidic chip.
- One Tygon^{TM} line connected through a metal canula to the outlet of the microfluidic chip on one end and to a 50 ml Falcon tube acting as a waste collector to the other.

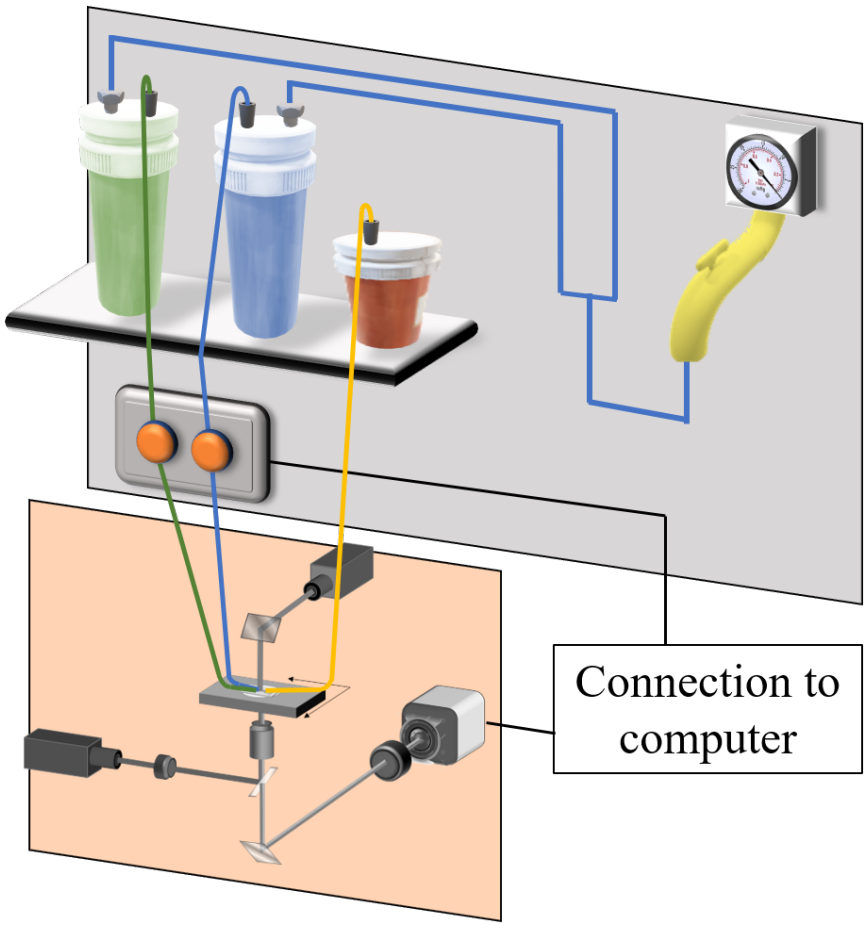

Figure 27: Outline of the fluid delivery system (grey wall) and its connections to the optical setup (orange wall). The pressure is provided by a wall faucet (in yellow) pumping pressurized gas through a Tygon^{TM} tube with a T-junction (in blue). The two endings reach the pressurized bottle and the pressurizing cap, which seals a falcon tube with the chemical to be tested. Both are connected to the arena through Tygon^{TM} going through two electrovalves (in red). Depending on which valve is open, the corresponding liquid will flow through a tube (green for the odorant, blue for the buffer) into the chip. It will fill the arena inside the microfluidic device and then will flow out from it through a dedicated tube (in yellow) to the trash reservoir (in orange).

When the system is in operation, the pressurizing cap is connected to a falcon filled with the solution to be tested. During the tests, the system switches between two configurations. In the first one, *c1*, the electrovalve controlling the buffer flow is open, while the electrovalve controlling the odorant flow is closed. This creates a constant flow of buffer liquid through the whole microfluidic chip. In the second configuration, *c2*, the electrovalve controlling the buffer flow is closed and the one controlling the odorant flow is open. This configuration fills the chip with the odorant solution. In both configurations the outflow of liquid from the chip is directed to the waste collector. During a test, the system starts in configuration *c1* and switches after 10 seconds to configuration *c2*. After 20 seconds, it switches back to configuration *c1* for 30 seconds again. To test a new solution, the falcon is replaced with an other one containing the new odorant to be analyzed and its liquid flow is activated for three minutes to wash away any remaining odour in the Tygon^{TM} tubes. Pressure, tube materials and dimensions are chosen considering the need of a rapid and complete switch between liquids and a low mechanical stress for the nematodes in the chip.

Filling time and dynamics of the microfluidic device have been measured through dye solutions and transmission recordings. Chemical responses have also been tested with fluorescence recordings of *C. elegans* responding to isoamyl alcohol at various concentrations within a range from 10^{-6} and 10^{-1}, which acts as an attractant eliciting activation of the AWC^{ON} neuron [42] upon removal.

After each experiment, fittings and canulae are cleaned in a six hour long alcohol bath followed by two 12 hour long baths in distilled water and then dried in oven at 60° C. The pressurized bottle and the pressurizing cap are sterilized in autoclave, while the Tygon^{TM} tubes are replaced for every new experiment.

5.6 Computer controls, GUI and post-processing

To synchronize the action of the optical setup and the fluid delivery system, we operate both electrovalves, the CMOS camera, and the two LEDs through a National Instruments I/O data acquisition mod-

ule controlled by a computer and set with a clock frequency of 0.1 s (see figure 28). We wrote a custom MATLAB^{TM} script [54] that allows to record videos and visualize the images acquired by the camera (activating either one of the two LEDs) in real time, and to open and close the electrovalves trough the NI device (see figure 29). In particular, the script generates a GUI (graphical user interface) that allows in a user-friendly manner to control the exposure time of the camera, to create a ROI in the visualized image, to capture a background image, and to set a defined time of exposure to the chemicals. With this software we also run the experimental action sequence, a set of commands passed by the computer to all controllable devices through the NI board, which we used to perform all chemical response testing during the experiments. The moving stage is controlled through a dedicated connection to the computer.

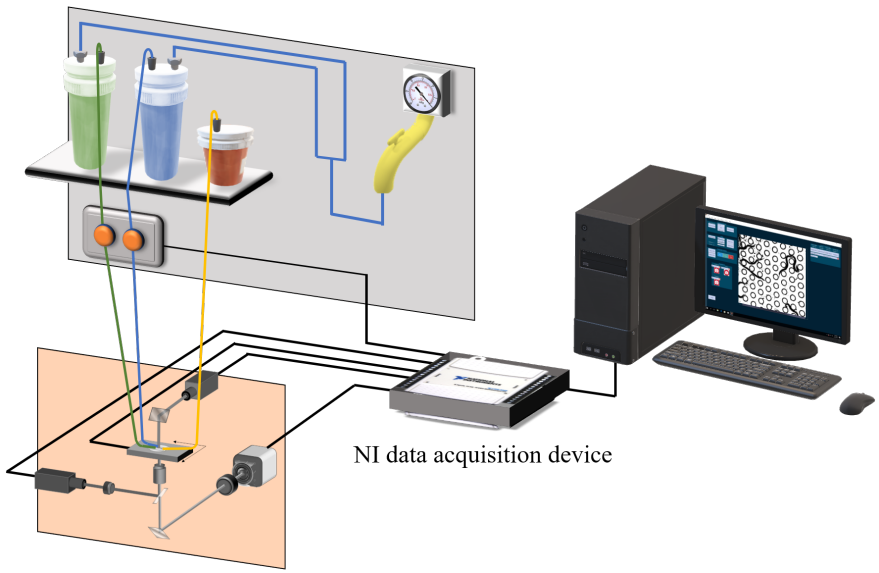

Figure 28: Outline of the connections between the acquisition devices and the computer. The National Instruments I/O data acquisition device allows to control the camera, the two LEDs and the moving stage of the optical setup (orange wall), as well as the electrovalves of the fluid delivery system (grey wall).

We used custom made MATLAB^{TM} scripts to perform image seg-

mentation, signal processing and data processing as well (see Figure 16). The scripts start by removing the mean of the first and last 5 frames, which are acquired in the dark to record background noise. It then applies an averaging filter to reduce noise and selects the frame acquired 2 seconds after the removal of the odor, in which the probability of having active neurons is higher. This frame is then shown to the user who can select the ROIs containing viable nematode heads. Nematodes that appear to have restrained access to the surrounding chemicals are discarded. In the following step the user is required to select the position of the neuron. With this information, the script tracks the neuron throughout the video in both temporal directions by looking for the maximum intensity averaged over a 5×5 pixels area that may not be more than 30 pixels away from the neuronal position assigned in the previously processed frame. The resulting signal intensity, I, is calculated as $I = \frac{\Delta F}{F_0}$, where $\Delta F = F - F_0$ and F_0 is the mean intensity of the neuron in the frames between seconds 5 and 10 of the acquisition. In case the neuron changes position in the ROI from a frame i to its next one $(i + 1)$, the element-wise sum of the intensity difference, $ID_{i,i+1}$, between the ROIs in the two frames will vary much more if compared to a still video. We thus apply a condition that identifies viable traces as those ones in which the aforementioned difference satisfies the following condition: $ID_{i,i+1} < \overline{ID_i} + \sigma_{ID_i}$, where $\overline{ID_i}$ and σ_{ID_i} are the mean value and the standard deviation respectively, calculated over all the IDs of the frames available in the range going from $i - 20$ to $i + 20$. If a viable signal is detected and visually validated, the standard deviation of the signal in a 10-second time-window starting from second 12, σ_{on}, is compared against the difference of the intensity of the signal averaged over a 10-second time-window starting from second 32, I_{off}, and the same quantity calculated in the time-window starting from second 12, I_{on}. If $I_{off} - I_{on} > 3\sigma_{on}$, the signal is assigned to post-removal "activation" (N_{act}), or "attraction". It is assigned to "no attraction" otherwise. Setting the threshold to $3\sigma_{on}$ guarantees that small amplitude responses, which may depend on shear stress sensed upon valve switching, are neglected. Once all traces have been assigned to either one of the two options, the script associates all experiments targeting

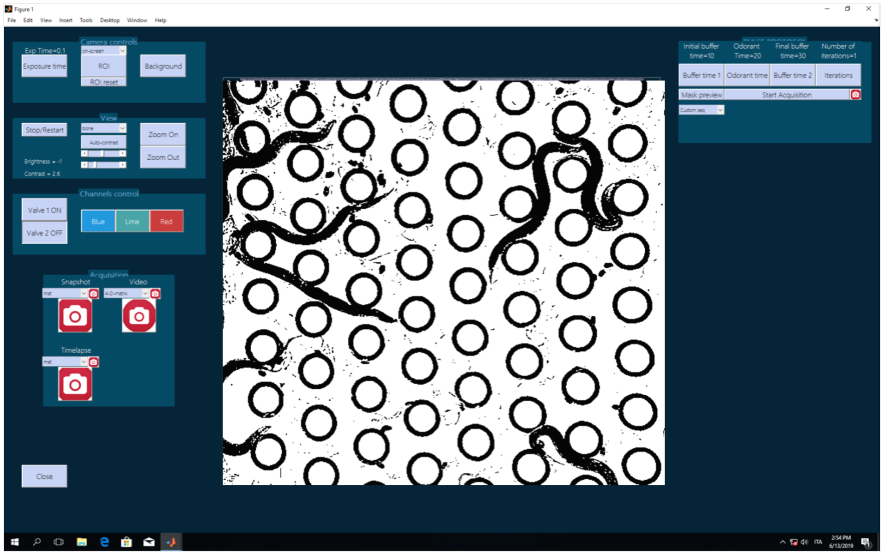

Figure 29: Screenshot of the graphic user interface (GUI) developed to control the instruments while running the experiments. It allows to activate the LEDs and the flow inside the chip through the electrovalves, to acquire images and time-lapses, to record videos, to set a custom experimental stimulation pattern for chemical response tests and to control the exposure time of the camera and the ROI of the visualized image.

the same sample and updates its corresponding NAI (reported in section 3), according to the following formula: $NAI = 2(N_{act}/N_{tot} - 1/2)$, where N_{act} is the number of signals associated to "attraction" and N_{tot} the total number of viable signals in all associated experiments.

5.7 Paralyzing solution administration and stocking

Nematodes in chip are paralyzed by filling the device with a solution of 0.24 mg of levamisole (Sigma-Aldrich) diluted in 1 ml of SBasal injected through the loading port. For 15 minutes after injection, the flow from the fluid delivery system is blocked, and inlets and outlets are clamped. After administration, young adults assume a rod-like posture and stop moving. At this point all clamps are removed and

the arena is washed in a constant SBasal flow. During the experiments levamisole is administered every time motion is impairing acquisitions. The paralyzing solution is produced every week and kept at 4° C.

5.8 Buffer solution preparation

In the chemical response experiments we used SBasal as the control solution, which does not elicit any kind of chemosensory response in the nematode. It is widely used as a buffer with *C. elegans* and its preparation is described in the following.

For a quantity of 500 ml of Sbasal, we mix 0.5 g of K_2HPO_4, 3 g of KH_2PO_4 and 2.925 g of NaCl with a magnetic stirrer in a bottle filled with 490 ml of distilled water. After the salts are dissolved, we add the 10 ml of distilled water making sure the PH of the solution is 6. Once the solution has the right acidity, it can be sterilized in the autoclave to be used for the experiments.

5.9 Urine solution preparation

To prepare the urine samples for chemical response experiments, we thaw at room temperature one aliquot for each sample to be tested. We take 20 µl of urine from each aliquot and dilute it in 2 ml of SBasal. We then filter the solution with a 0.22 µm filter, put it in a falcon tube and place it in a container filled with ice, waiting for the experiments to begin.

5.10 *C. elegans* preparation

For upcoming experiments, *C. elegans* are thawed, synchronized and kept in culture so that they reach the young adult stage at the day of the experiments. Before being tested, the nematodes are washed from bacteria and loaded onto the microfluidic device. These steps will be explained in the following paragraphs.

To prepare the *C. elegans* for testing, we pick about 25 young adults from the culture plate and put them on a 35 mm petri dish. We

then wash the petri dish with about 1.5 ml of SBasal, tilting it to make sure all nematodes get trapped inside the solution. After picking up the liquid and all nematodes inside of it with a glass pipette, we put it in a 1.5 ml tube. Here, we perform two washes in SBasal and a wash in distilled water. To wash the solution, we wait three minutes, or until all nematodes are not suspended in the solution anymore, and replace the liquid volume above the nematodes with new, clean solution.

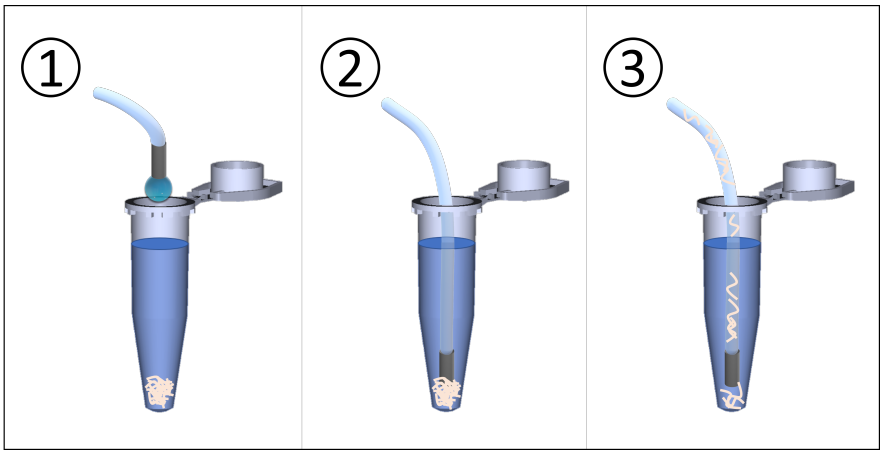

Figure 30: To load the animals onto the arena, we use a Tygon™ tube attached to a metal canula at one end, and to a 1 ml syringe at the other. After filling the Tygon™ tube with distilled water and forming a drop at its open end (1), we insert it in the water (2) and pick up the nematodes from the bottom of the 1.5 ml tube (3), paying attention to keep them inside the Tygon™ tube 30. Any animal that reaches the syringe is lost, and can hardly be pushed inside the microfluidic device.

To load the animals onto the microfluidic device, we use an 80 cm long Tygon™ tube with the same characteristics of the ones used for the fluid delivery system attached to a metal canula at one end, and to a 1 ml syringe at the other. After filling the Tygon™ tube with distilled water, we pick up the nematodes from the bottom of the 1.5 ml tube, paying attention to keep them inside the Tygon™ tube (see figure 30). Any animal that reaches the syringe is lost, and

can hardly be pushed inside the microfluidic device. We then attach the Tygon^{TM} filled with *C. elegans* to the loading port of the chip applying the drop-to-drop technique. With no flow inside the chip, we gently inject the liquid by pushing the plunger on the syringe, trying to avoid clustering of the animals in either the loading port, the tampered channel leading to the arena, or at the entrance of the arena. Once the nematodes are inside the chip, we let them adapt to the new environment for 20 minutes.

5.11 Urine sample collecting and stocking

Urine samples are collected in the morning from patients in hospital facilities. They are delivered as soon as possible in 5 ml falcons in an ice filled polyester box to our laboratories. The samples are then filtered with a 0.2 μm syringe filter and divided in at least 10 aliquots of 100 μl each and stored in 200 μl tubes at -80° C to limit molecule degradation.

Each aliquot is tested multiple times with different nematodes during one experimental run and then discarded. Before testing, urine samples are diluted to get a 10^{-2} urine concentration in buffer solution. During testing, the liquid reservoirs are placed in an ice filled container to avoid heating of the odorants.

5.12 Urine testing

Urine testing has been performed on 36 cancer patients and 36 control samples. Each day of experiment, we test 4 urine samples from cancer patients and 4 control samples. Each sample is tested at least two times in two different days. Nematodes are kept in testing environment for no more than 3 hours. The following paragraphs describe how to perform the experiments to assess *C. elegans* response towards chemical stimuli.

Before starting the experiments, we make sure that we have a synchronized population of PS6374 *C. elegans* strain at the young adult stage (see section 5.1), at least two microfluidic devices, the buffer solution and the paralyzing solution, prepared following sections 5.3,

5.8, and 5.7 respectively. To start the experiments, we prepare the microfluidic device following the procedures described in section 5.3 and connect it to the fluid delivery system (see section 5.5). After having set the right pressure for a gentle flow inside the arena, we wash about 25 nematodes of the PS6374 line and load them onto the device according to the steps reported in section 5.10. We let the animals adapt and roam in the new environment for 20 minutes under constant buffer flow. Once they are equally distributed inside the chip, we proceed to levamisole administration following the steps described in section 5.7. While waiting for the nematodes to fully paralyze, we dilute the urine samples to be tested according to the steps reported in section 5.9. Once the solutions are ready, we load the chip on the moving stage of the optical setup (see section 5.2) and visualize the inside of the arena to make sure that the nematodes are healthy and no air is inside the microfluidic device.

The first test is a control check in which we assess preference of nematodes towards SBasal vs. itself. In this case, should the nematodes show significant responses upon flow switching, it might either be due to the fact that the chip is dirty, and bacterial residues have entered the arena, or that the flow is too strong, eliciting a pressure response in the AWC^{ON} neuron. If the test goes well, we proceed to urine sample testing, replacing the SBasal in the testing position with the first urine sample to be tested. Otherwise, we clean the chip and adjust the pressure until we see no significant response in the SBasal tests. During the test, we first position the moving stage so that we have about half of the nematodes in the field of view, excluding animals that have possible hindrance to surrounding chemical sensing. We make sure that no AWC^{ON} neuron is active, and then start the acquisition procedure described in section 5.2. Once the acquisition is over, we wait for some time until all neurons are quiescent, and move to a new area of the arena to measure the response of other animals. When all animals have been tested, we switch to a new sample, washing the residues of the previous one as described in section 5.5.

At the end of the experiments, we trash all urine samples, all Tygon^{TM} tubes and any consumable used. We sterilize the arena and trash it as well, and clean the pressurized bottle, the pressurizing cap,

all fittings and canulae according to section 5.5. For each experiment, we register the temperature of the room, the number and stage of nematodes inside the chip, the time they spent in the arena and the time of paralyzing solution administration, as well as any kind of problem encountered during the experiments.

6 Troubleshooting

This section lists all problems encountered during the calibration of our setup, during the preparation of the experiments and during the experiments themselves. They are related to either the microfluidic environment, or to the nematodes, their responses and their calcium indicators, or to the urine sample solutions.

6.1 Problems related to the microfluidic environment

- Air bubbles: one of the events that may invalid experiments, is the introduction of air bubbles inside the chip. Air bubbles prevent a uniform distribution of the chemicals injected inside the arena, possibly leading to false negatives. Additionally, *C. elegans* may dry out and die if exposed to air-only environments. To avoid the presence of air inside the chip, it is very important to degas it before beginning the experiments and to perform the first connection between the fluid delivery system and the microfluidic device in water, while all following ones need to be performed with a with a drop-to-drop technique. Before loading the animals onto the device, it is also advisable to leave it under a constant flow for about 20 minutes, switching the flow a few times. The mechanical stress produced by the activation of the electrovalves may let any air bubble trapped inside the cables detach from the inner walls of the tubes so that it can get flushed away by the constant flow. In any case, experiments have to be stopped as soon as bubbles are detected inside the chip, unless their size is small enough to avoid affecting the operating conditions of the setup, and their position is not disrupting correct flow distribution. To get rid of bubbles,

we either leave the chip under a constant flow for some minutes, or carefully disconnect the problematic lines of the fluid delivery system. We then fill them again with liquid and attach them back to the rest of the lines using the drop-to-drop technique. If air bubbles stop inside tube fittings, we gently tap on the corresponding parts until the air comes off from it and let it flow out by opening the next available connection in the flow supply line.

- Pressure response: an additional issue affecting the validity of our experiments is related to the sensitivity of the AWC^{ON} neuron with respect to mechanical stimuli. In some cases, flow switch elicits a neuronal response that is significantly smaller than the chemical one, and is due to mechanosensation. It is still unclear whether the response is generated by the neuron itself or if it is transmitted to it from other ones. To prevent this from happening, we usually try many different solutions. First of all, we reduce the pressure to the lowest possible one that can rapidly fill the arena. In this way, the switch creates a smaller shockwave inside the tubes. Secondly, we test only animals whose position is not affected too much by the flow switch. Animals that upon switching touch other animals, or elements inside the arena, will likely show a mechanosensory response. Finally, before beginning any experimental run, we record the response of the animal towards a flow switch between two buffer flows. In this case, the chemical response should be completely abolished, allowing us to see how strong the mechanosensory response is. If it is in a range that does not disrupt the outcome of the experiments, we proceed to the chemical testing. Otherwise, we adjust the pressure and the distribution of the animals until these unwanted responses are abolished or lowered in as many animals as possible. An other solution, which showed good results, is the use of rotating servo actuators (instead of electrovalves), which avoid an abrupt closing of the channels, preventing the creation of a shockwave inside the arena. However, this makes the diffusion of the injected liquid inside the arena slower. Because of this, we adopted such a solution only

in those cases in which we could not significantly lower the pressure response from the AWC^{ON} neurons.

- Dirty chip: one of the other problems that may depend on the microfluidic device occurs when the nematodes respond to the SBasal-SBasal switch as they do when sensing attractants. When this happens, it may depend on the chip in use, because it might retain some dirt from previous experiments. We tried many different protocols for chip cleaning and no one proved to be completely effective. The best protocol involves the removal of *C. elegans* from the chip and residual odors by injecting bleach for 5 minutes and then soaking it in alcohol overnight. However, these procedures may alter the transparency and elastic properties of the PDMS and do not assure a complete removal of the odors inside the chip. To remove dependency on previously tested odorants, we resorted to making a new chip for every new experiment.

- Design of the arena: the nematode barrier and the confinement of the *C. elegans* in the field of view. The design of the arena has to take into account the field of view of the optical setup, which depends on the camera and the objective in use. It is preferable to limit the number of acquisitions required to record the response from all animals. Multiple acquisitions mean multiple stimulation of all animals in the arena, regardless if they are in the field of view or not. The response seems to not change upon multiple presentation of the same stimulus, however, bleaching may affect later recordings, yielding altered results. The worm barrier placed at the entrance and at the exit of the arena has to take into account the size of the inspected animals and the fact that the PDMS polymer may deform under mechanical stress. If the fluid in the arena is too strong, nematodes may cross the nematode barrier reaching the waste reservoir. Any animal that leaves the arena is lost.

- Clogged outflow channels: the nematode barriers may sometimes get clogged by *C. elegans*. This usually happens when

the inflow of liquid is too high, pushing the animals towards the outlet. If the outflow is clogged, odour switching cannot be granted in the whole arena. This can create false outcomes during the response tests, due to the mechanosensation of pressure changes related to obstructed outlets or to a non-uniform distribution of the odorant. It is therefore suggested to stop the experiment and to solve the issue before continuing. To remove the animals blocked in the worm barriers, it is advisable to detach one of the injection tubes from the inlet and to close the inlet port by attaching it to a Tygon^{TM} tube, which can be clamped after being connected and filled with liquid. The injection tube can now be connected to the outlet port. In this configuration, the direction of the flow can be inverted by opening the valve controlling the tube connected to the outlet port and closing the other one. When doing so, it is important to remember to unclamp the Tygon^{TM} tube attached to the loading port, which will serve as the outlet. The inversion of the flow will push the animals outside the worm barriers. Once this happens, everything can be reverted to the standard configuration but the pressure needs to be lowered, to prevent the problem from occurring again.

- Clogged loading channel: the loading channel can get clogged by either some debris from the petri dish in which the *C. elegans* are contained before the washing or through the animals themselves if the loading tube is too crowded. In such a case, we can first try to push the clogging element through the loading channel: if it is a small debris it will be flushed away upon flow activation while *C. elegans* may separate to go through the channel and stop at the entrance of the arena once inside. At this point we need to wait for the entrance to be free again before loading any additional animal. If the loading channel is completely clogged we can try to push the clogging element towards the loading port, in the opposite direction of the liquid flow. We can do this by sucking from the syringe or by attaching the flow supply tubes to the outlet port and activating the flow. In case the channel cannot be cleared the loading can-

not be completed. It is suggested to either start the experiments with the already loaded animals or to start over with a new chip.

6.2 Problems related to the *C. elegans*

- Low GCaMP expression: the nematodes sometimes show a very low fluorescence signal. This is due to the fact that new generations gradually loose the expression of the calcium indicator. To prevent this from happening, it is suggested to thaw new animals from the original line and produce a synchronized population every three/four weeks.

- Bleaching: too high LED power causes bleaching of the calcium indicators. We set the power as low as possible to detect calcium transients and use pulsed excitation during imaging. This allows to keep a relatively high fluorescence signal throughout the experiment. It is worth to notice that too high LED power is not recommended also because it can trigger a photosensitive reaction in the animal.

- Fluorescent intestines: fluorescence may spread over other parts of *C. elegans* body. Intestines in particular may show a relatively high fluorescence. In the worst cases, this problem produces a wrong image segmentation, resulting in wrong signal extraction. To avoid this, our automated signal-processing is designed to proceed in a supervised fashion. While slowing down post-processing, this allows to remove artifacts that cannot be easily distinguished from the real signal.

- Loading problems: while doing the loading, it is advisable to use a long Tygon^{TM} tube to collect the nematodes from the washing tube. This is important because, whenever the animals reach the syringe while being drawn from the washing solution, they are inevitably trapped inside it. If this happens, the only solution is to prepare a new group of *C. elegans* for the experiment. The use of a long tube allows to have more space to collect remaining nematodes avoiding that those ones already

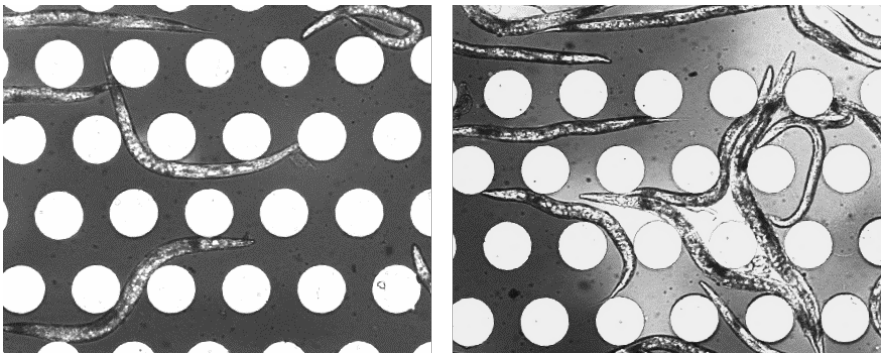

Figure 31: An example of a complete chemical distribution of 1 millimolar xylene cyanol (left), and an incomplete one (on the right), in which the chemical does not reach the nose tip of clustered animals at the intended concentration (dark areas are have the right concentration, brighter ones do not). These animals will yield an altered response with respect to the surrounding ones, due to the odorant inaccessibility.

in the tube reach the syringe. Additionally, it is important to keep track of the animals inside the tube.

- Clustering problems: when the loading is done, it is suggested to wait some time to let the animals explore the arena. In the event that the animals are clustered in small areas, a way to make them spread out inside the environment is to exploit photosensitivity by shining on them a light, if they are not paralyzed. If this not the case, it is better to discard clustered animals from the analysis, as the distribution of the chemical cannot be granted inside nematodes clusters. Figure 31 shows an example of a complete chemical distribution of 1 millimolar xylene cyanol (left), and an incomplete one (on the right), in which the chemical does not reach the nose tip of all animals at the intended concentration. Situations like this inevitably alter the evaluation of the *NAI*.

- Paralyzing problems: the paralyzing solution makes the animals contract body wall muscles until they reach a stiff, rod-

like posture. During levamisole injection, it may happen that the chemical elicits a too strong muscle contraction that breaks the integrity of some *C. elegans*, making the intestines come out from the vulva. When this happens, the surrounding area is filled in a fluorescent liquid, reducing the signal to noise ratio of the neuronal signals and producing odors that may alter the response from other nematodes. To prevent this from happening, it is advisable to inject the paralyzing solution as slow as possible, to limit mechanical stress on cuticles, and to keep an eye on the integrity of all nematodes inside the chip. If any of them seems to suffer from the injection, it is better to make a pause, or to slow down.

6.3 Problems related to the urine samples

- Varying responses. The response to previously thawed and refrozen urine samples gradually shifts towards values related to attraction. This is due to a possible proliferation of bacteria inside the sample or to the degradation of macromolecules that can create "chemical noise" in the array of chemicals to be sensed by *C. elegans*. To limit this phenomenon, as soon as we collect a sample, we divide it into 10 aliquots and thaw them all. Each time we test a sample, we take one aliquot and trash it. Any further test on the same sample will be carried out on a new aliquot.

References

[1] S. Brenner, "The genetics of caenorhabditis elegans," *Genetics*, vol. 77, no. 1, pp. 71–94, 1974.

[2] J. E. Sulston, E. Schierenberg, J. G. White, and J. Thomson, "The embryonic cell lineage of the nematode caenorhabditis elegans," *Developmental biology*, vol. 100, no. 1, pp. 64–119, 1983.

[3] M. A. Herman, "Hermaphrodite cell-fate specification," 2006.

[4] J. G. White, E. Southgate, J. N. Thomson, and S. Brenner, "The structure of the nervous system of the nematode caenorhabditis elegans: the mind of a worm," *Phil. Trans. R. Soc. Lond*, vol. 314, pp. 1–340, 1986.

[5] T. B. Achacoso and W. S. Yamamoto, *AY's Neuroanatomy of C. elegans for Computation*. CRC Press, 1991.

[6] R. M. Durbin, "Studies on the development and organisation of the nervous system of caenorhabditis elegans," 1987.

[7] L. R. Varshney, B. L. Chen, E. Paniagua, D. H. Hall, and D. B. Chklovskii, "Structural properties of the caenorhabditis elegans neuronal network," *PLoS computational biology*, vol. 7, no. 2, p. e1001066, 2011.

[8] Z. F. Altun, L. A. Herndon, C. A. Wolkow, C. Crocker, R. Lints, and D. H. Hall, "Wormatlas," *http://www.wormatlas.org*, 2002-2019.

[9] L. B. Buck, "The olfactory multigene family," *Current opinion in genetics & development*, vol. 2, no. 3, pp. 467–473, 1992.

[10] A. Chess, I. Simon, H. Cedar, and R. Axel, "Allelic inactivation regulates olfactory receptor gene expression," *Cell*, vol. 78, no. 5, pp. 823–834, 1994.

[11] R. Vassar, J. Ngai, and R. Axel, "Spatial segregation of odorant receptor expression in the mammalian olfactory epithelium," *Cell*, vol. 74, no. 2, pp. 309–318, 1993.

[12] B. Vidal, U. Aghayeva, H. Sun, C. Wang, L. Glenwinkel, E. A. Bayer, and O. Hobert, "An atlas of caenorhabditis elegans chemoreceptor expression," *PLoS biology*, vol. 16, no. 1, p. e2004218, 2018.

[13] C. I. Bargmann, "Chemosensation in c. elegans," 2006.

[14] R. L. Doty, *Handbook of olfaction and gustation*. John Wiley & Sons, 2015.

[15] T. Hirotsu, H. Sonoda, T. Uozumi, Y. Shinden, K. Mimori, Y. Maehara, N. Ueda, and M. Hamakawa, "A highly accurate inclusive cancer screening test using caenorhabditis elegans scent detection," *PLoS One*, vol. 10, no. 3, p. e0118699, 2015.

[16] M. Duffy, N. Harbeck, M. Nap, R. Molina, A. Nicolini, E. Senkus, and F. Cardoso, "Clinical use of biomarkers in breast cancer: Updated guidelines from the european group on tumor markers (egtm)," *European journal of cancer*, vol. 75, pp. 284–298, 2017.

[17] X. Chen, Y. Yuan, Z. Gu, and K. Shen, "Accuracy of estrogen receptor, progesterone receptor, and her2 status between core needle and open excision biopsy in breast cancer: a meta-analysis," *Breast cancer research and treatment*, vol. 134, no. 3, pp. 957–967, 2012.

[18] E. Moser and M. McCulloch, "Canine scent detection of human cancers: A review of methods and accuracy," *Journal of Veterinary Behavior*, vol. 5, no. 3, pp. 145–152, 2010.

[19] M. McCulloch, T. Jezierski, M. Broffman, A. Hubbard, K. Turner, and T. Janecki, "Diagnostic accuracy of canine scent detection in early-and late-stage lung and breast cancers," *Integrative cancer therapies*, vol. 5, no. 1, pp. 30–39, 2006.

[20] H. Sonoda, S. Kohnoe, T. Yamazato, Y. Satoh, G. Morizono, K. Shikata, M. Morita, A. Watanabe, M. Morita, Y. Kakeji, *et al.*, "Colorectal cancer screening with odour material by canine scent detection," *Gut*, vol. 60, no. 6, pp. 814–819, 2011.

[21] K. Matsumura, M. Opiekun, H. Oka, A. Vachani, S. M. Albelda, K. Yamazaki, and G. K. Beauchamp, "Urinary volatile compounds as biomarkers for lung cancer: a proof of principle study using odor signatures in mouse models of lung cancer," *PloS one*, vol. 5, no. 1, p. e8819, 2010.

[22] J. Nakai, M. Ohkura, and K. Imoto, "A high signal-to-noise ca 2+ probe composed of a single green fluorescent protein," *Nature biotechnology*, vol. 19, no. 2, p. 137, 2001.

[23] R. Yasuda, E. A. Nimchinsky, V. Scheuss, T. A. Pologruto, T. G. Oertner, B. L. Sabatini, and K. Svoboda, "Imaging calcium concentration dynamics in small neuronal compartments," *Sci. STKE*, vol. 2004, no. 219, pp. pl5–pl5, 2004.

[24] Y. Yamada and K. Mikoshiba, "Application of genetically encoded indicators to mammalian central nervous system," *Frontiers in molecular neuroscience*, vol. 8, p. 76, 2015.

[25] J. Akerboom, J. D. V. Rivera, M. M. R. Guilbe, E. C. A. Malavé, H. H. Hernandez, L. Tian, S. A. Hires, J. S. Marvin, L. L. Looger, and E. R. Schreiter, "Crystal structures of the gcamp calcium sensor reveal the mechanism of fluorescence signal change and aid rational design," *Journal of biological chemistry*, vol. 284, no. 10, pp. 6455–6464, 2009.

[26] P. Gravesen, J. Branebjerg, and O. S. Jensen, "Microfluidics-a review," *Journal of micromechanics and microengineering*, vol. 3, no. 4, p. 168, 1993.

[27] A. San-Miguel and H. Lu, "Microfluidics as a tool for c. elegans research," 2013.

[28] N. Chronis, "Worm chips: microtools for c. elegans biology," *Lab on a Chip*, vol. 10, no. 4, pp. 432–437, 2010.

[29] K. Chung, M. M. Crane, and H. Lu, "Automated on-chip rapid microscopy, phenotyping and sorting of c. elegans," *Nature methods*, vol. 5, no. 7, p. 637, 2008.

[30] K. Chung, M. Zhan, J. Srinivasan, P. W. Sternberg, E. Gong, F. C. Schroeder, and H. Lu, "Microfluidic chamber arrays for whole-organism behavior-based chemical screening," *Lab on a Chip*, vol. 11, no. 21, pp. 3689–3697, 2011.

[31] H. Lee, M. M. Crane, Y. Zhang, and H. Lu, "Quantitative screening of genes regulating tryptophan hydroxylase transcription in caenorhabditis elegans using microfluidics and an adaptive algorithm," *Integrative Biology*, vol. 5, no. 2, pp. 372–380, 2012.

[32] A. Ben-Yakar and F. Bourgeois, "Ultrafast laser nanosurgery in microfluidics for genome-wide screenings," *Current Opinion in Biotechnology*, vol. 20, no. 1, pp. 100–105, 2009.

[33] D. R. Albrecht and C. I. Bargmann, "High-content behavioral analysis of caenorhabditis elegans in precise spatiotemporal chemical environments," *Nature methods*, vol. 8, no. 7, p. 599, 2011.

[34] J. Larsch, D. Ventimiglia, C. I. Bargmann, and D. R. Albrecht, "High-throughput imaging of neuronal activity in caenorhabditis elegans," *Proceedings of the National Academy of Sciences*, vol. 110, no. 45, pp. E4266–E4273, 2013.

[35] L. Tian, S. A. Hires, T. Mao, D. Huber, M. E. Chiappe, S. H. Chalasani, L. Petreanu, J. Akerboom, S. A. McKinney, E. R. Schreiter, *et al.*, "Imaging neural activity in worms, flies and mice with improved gcamp calcium indicators," *Nature methods*, vol. 6, no. 12, p. 875, 2009.

[36] N.-T. Nguyen, S. T. Wereley, and S. A. M. Shaegh, *Fundamentals and applications of microfluidics*. Artech house, 2019.

[37] Y. Xia and G. M. Whitesides, "Soft lithography," *Annual review of materials science*, vol. 28, no. 1, pp. 153–184, 1998.

[38] E. R. Troemel, A. Sagasti, and C. I. Bargmann, "Lateral signaling mediated by axon contact and calcium entry regulates asymmetric odorant receptor expression in c. elegans," *Cell*, vol. 99, no. 4, pp. 387–398, 1999.

[39] P. D. Wes and C. I. Bargmann, "C. elegans odour discrimination requires asymmetric diversity in olfactory neurons," *Nature*, vol. 410, no. 6829, p. 698, 2001.

[40] S. H. Chalasani, N. Chronis, M. Tsunozaki, J. M. Gray, D. Ramot, M. B. Goodman, and C. I. Bargmann, "Dissecting a circuit for olfactory behaviour in caenorhabditis elegans," *Nature*, vol. 450, no. 7166, p. 63, 2007.

[41] S. E. Worthy, L. Haynes, M. Chambers, D. Bethune, E. Kan, K. Chung, R. Ota, C. J. Taylor, and E. E. Glater, "Identification of attractive odorants released by preferred bacterial food found in the natural habitats of c. elegans," *PloS one*, vol. 13, no. 7, p. e0201158, 2018.

[42] A. Zaslaver, I. Liani, O. Shtangel, S. Ginzburg, L. Yee, and P. W. Sternberg, "Hierarchical sparse coding in the sensory system of caenorhabditis elegans," *Proceedings of the National Academy of Sciences*, vol. 112, no. 4, pp. 1185–1189, 2015.

[43] K. Yoshida, T. Hirotsu, T. Tagawa, S. Oda, T. Wakabayashi, Y. Iino, and T. Ishihara, "Odour concentration-dependent olfactory preference change in c. elegans," *Nature communications*, vol. 3, p. 739, 2012.

[44] P. Sengupta, H. Colbert, B. Kimmel, N. Dwyer, and C. I. Bargrnann, "The cellular and genetic basis of olfactory responses in caenorhabditis elegans," *1993), The Molecular Basis of Smell and Taste Transduction*, pp. 235–250, 1993.

[45] S. Kato, Y. Xu, C. E. Cho, L. Abbott, and C. I. Bargmann, "Temporal responses of c. elegans chemosensory neurons are preserved in behavioral dynamics," *Neuron*, vol. 81, no. 3, pp. 616–628, 2014.

[46] M. P. Coleman, M. Quaresma, F. Berrino, J.-M. Lutz, R. De Angelis, R. Capocaccia, P. Baili, B. Rachet, G. Gatta, T. Hakulinen, *et al.*, "Cancer survival in five continents: a worldwide population-based study (concord)," *The lancet oncology*, vol. 9, no. 8, pp. 730–756, 2008.

[47] S. Iwanir, R. Ruach, E. Itskovits, C. O. Pritz, E. Bokman, and A. Zaslaver, "Irrational behavior in c. elegans arises from asymmetric modulatory effects within single sensory neurons," *Nature communications*, vol. 10, no. 1, p. 3202, 2019.

[48] R. D. Luce, *Individual choice behavior: A theoretical analysis*. Courier Corporation, 2012.

[49] T. Schrödel, R. Prevedel, K. Aumayr, M. Zimmer, and A. Vaziri, "Brain-wide 3d imaging of neuronal activity in caenorhabditis elegans with sculpted light," *Nature methods*, vol. 10, no. 10, p. 1013, 2013.

[50] R. Prevedel, Y.-G. Yoon, M. Hoffmann, N. Pak, G. Wetzstein, S. Kato, T. Schrödel, R. Raskar, M. Zimmer, E. S. Boyden, *et al.*, "Simultaneous whole-animal 3d imaging of neuronal activity using light-field microscopy," *Nature methods*, vol. 11, no. 7, p. 727, 2014.

[51] V. Venkatachalam, N. Ji, X. Wang, C. Clark, J. K. Mitchell, M. Klein, C. J. Tabone, J. Florman, H. Ji, J. Greenwood, *et al.*, "Pan-neuronal imaging in roaming caenorhabditis elegans," *Proceedings of the National Academy of Sciences*, vol. 113, no. 8, pp. E1082–E1088, 2016.

[52] I. Kotera, N. A. Tran, D. Fu, J. H. Kim, J. B. Rodgers, and W. S. Ryu, "Pan-neuronal screening in caenorhabditis elegans

reveals asymmetric dynamics of awc neurons is critical for thermal avoidance behavior," *Elife*, vol. 5, p. e19021, 2016.

[53] I. A. Hope, *C. elegans: a practical approach*, vol. 213. OUP Oxford, 1999.

[54] MATLAB, *version 9.5 (R2018B)*. Natick, Massachusetts: The MathWorks Inc., 2018.

A Calcium Imaging Protocol

Items needed

- Synchronized population of PS6374 *C. elegans* strain at the young adult stage
- 2 degassed microfluidic devices
- Buffer solution
- Paralyzing solution
- Working fluid delivery system
- Optical setup
- Ice box
- 4 clamps
- 2 sterile 1 ml syringes
- A 60 cm long Tygon^{TM} tube with a canula at one end
- A 5 cm long Tygon^{TM} tube with a canula at one end

Preparation

- Fill the buffer reservoir and the odorant reservoir with buffer
- Connect one of the degassed microfluidic devices to the fluid delivery system with the drop-to-drop technique
- Attach the 5 cm long Tygon^{TM} tube to the loading port to prevent formation of air bubbles inside the chip
- Check the tubes for any residual air bubble and, if present, let them flow out under mechanical stimulation
- Load the microfluidic device on the moving stage and inspect it for damages. If the chip is not intact, substitute it

- Adjust pressure to produce 1 droplet per second in the trash reservoir and let the buffer flow to wash the arena
- Wash about 25 nematodes of the PS6374 line and load them into the 60 cm Tygon™ tube through a 1 ml syringe
- Detach the short Tygon™ tube from the loading port and let a drop of water flow out from it
- Stop the buffer flow
- Connect the Tygon™ tube containing the nematodes to the loading port and load them into the device by gently pushing the plunger, following the movement of the nematodes inside the tube. When the nematodes are about to enter the arena, monitor their movement using the transmission image stream of the optical setup
- Activate the buffer flow and check the movement of the nematodes. If the nematodes are pushed to the barriers at the end of the arena, lower the pressure to a value that does not affect the nematodes location while still producing 1 droplet per second in the trash reservoir
- Let the nematodes adapt and roam in the new environment for 20 minutes under constant buffer flow checking the transmission images from time to time
- Once equally distributed, detach the loading tube and let a drop of liquid flow out from the loading port
- Attach the 5 cm long Tygon™ tube to a 1 ml syringe filled with levamisole solution
- Stop the buffer flow
- Attach the levamisole injection tube to the loading port
- Clamp the buffer injection tube and the odorant injection tube at their very end, close to the chip

- Inject 0.4 ml of the levamisole solution while monitoring the nematodes conditions through the transmission channel streaming
- Clamp the outlet tube and the levamisole injection tube and wait for 15 minutes

Experiment

1. Check the location of the nematodes. If they cluster at the end of the arena the pressure is too high and needs to be lowered to a value that does not affect their location while still producing 1 droplet per second in the trash reservoir
2. Check that the buffer reservoir and the odorant reservoir contain a sufficient amount of buffer (about 5 ml)
3. Move the stage to have half of the loaded nematodes in the field of view
4. Avoid nematodes that cannot sense surrounding chemicals because of barriers or because of the close presence of other animals
5. Select a region of interest in the field of view containing the heads of all visible nematodes
6. Start the experimental action sequence with SBasal as odorant
7. Move the stage to the other portion of the arena
8. Select a new region of interest in the field of view containing the remaining heads
9. Check the acquired videos and look for responses in AWC. If there are high responses at the flow switch in some of the nematodes but not all of them, adjust the flow. If all nematodes respond, there may be bacteria in the SBasal or in the tubes, in which case either one or both of them need to be replaced

10. Once the high responses to SBasal are absent, fill the odorant reservoir tube with the first urine dilution.
11. Wait for repolarization time of the neurons to be over
12. Move the stage to have half of the loaded nematodes in the field of view
13. Select a region of interest in the field of view containing the heads
14. Start the acquisition and wait for repolarization time
15. Wait for repolarization time of the neurons to be over
16. Move the stage to the other portion of the arena
17. Select a new region of interest in the field of view containing the remaining heads
18. Start the second acquisition and wait for repolarization time again
19. Stop the flow
20. Replace the odorant reservoir tube with a new urine sample
21. Repeat steps 11-20 for every urine sample to be tested
22. Stop the flow and dispose of everything

B Ethics committee approval

The study was approved by the research ethics committee of "Fondazione Santa Lucia", Italy. The following page reports the document of approval of this study.

Comitato Etico Indipendente

SANTA LUCIA
NEUROSCIENZE E RIABILITAZIONE

Prof. Giancarlo Ruocco
Fondazione Istituto Italiano di Tecnologia
Sede

Prot. CE/PROG.621 13-07-17

Visti gli atti propri del Comitato Etico operante presso la Fondazione Santa Lucia di Roma, con sede in Via Ardeatina 306, 00179 Roma

Si comunica

in data 10 luglio 2017 si è svolta la riunione del Comitato Etico, durante la quale è stata esaminata tra l'altro, la proposta da Lei avanzata per il progetto dal titolo **"Studio della risposta neuronale del circuito olfattorio nel C.elegans per l'analisi della presenza di metaboliti tumorali in campioni di urine".**

Dopo la discussione il Comitato ha deciso di approvare lo studio all'unanimità.

Distinti Saluti.

FONDAZIONE SANTA LUCIA - COMITATO ETICO - I.R.C.C.S.

Per la Segreteria
Elisa Battisti

Fondazione Santa Lucia IRCCS
Via Ardeatina 306, 00179 Roma
T +39 06 5150 11 F +39 06 5032 097

C.F. 97138260589 P.Iva 05692831000
www.fondazionesantalucia.it